Master's Thesis of Agriculture

Polyethylenimine-conjugated Hydroxyethyl Cellulose for Doxorubicin/Bcl-2 siRNA Co-delivery Systems

Doxorubicin/Bcl-2 siRNA 동시 전달을 위한 폴리에틸렌이민으로 개질한 하이드록시에틸셀룰로오스 전달체 개발

February 2023

Graduate School of Agriculture and Life Sciences
Seoul National University
Department of Agriculture, Forestry and Bioresources

Jiwon Park

Polyethylenimine-conjugated Hydroxyethyl Cellulose for Doxorubicin/Bcl-2 siRNA Co-delivery Systems

Advised by Prof. Tae-il Kim

Submitting a master's thesis of
Agriculture

November 2022

Graduate School of Agriculture and Life Sciences
Seoul National University
Department of Agriculture, Forestry and Bioresources

Jiwon Park

Confirming the master's thesis written by
Jiwon Park
January 2023

Chair Chang Seok Ki (Seal)

Vice Chair Tae-il Kim (Seal)

Examiner Sungchul Shin (Seal)

Abstract

Hydroxyethyl cellulose (HEC), widely known for its biocompatibility and water solubility, is a potential material for pharmaceutical use, especially in delivery systems. Here, we synthesized polyethylenimine (PEI)-conjugated hydroxyethyl cellulose (HECP2k) and evaluated HECP2k as a novel gene/drug carrier. HECP2k was synthesized by reductive amination with PEI and oxidized HEC. Using ^{1}H NMR, the molar amounts of primary amine were calculated to 2.7, 5.2, and 7.0 mmole/g for HECP2k 1X, 5X, and 10X, respectively. Also, by primary amine quantification, the molar amounts of primary amine were double-checked to 1.48, 2.13, and 3.86 mmole/g for HECP2k 1X, 5X, and 10X. The weight average molecular weights were measured as 13.92, 9.38, and 7.27 kDa for HECP2k 1X, 5X, and 10X, respectively. pDNA condensing ability of HECP2k increased as the PEI conjugation ratio increased. HECP2k/pDNA polyplexes retained the size of 100–300 nm while their zeta-potential was about 30 mV. Although HECP2k 1X showed a bit of cytotoxicity, HECP2k 5X and 10X showed above 90% of relative cell viability. In the transfection test, HECP2k 10X/pDNA polyplex with the optimized weight ratio exhibited 35–127 times enhanced efficiency than the positive control in serum-free condition, and 9-19 times enhanced efficiency in serum condition. HECP2k 10X was optimized to the experimental group (HECP2k) for the following experiments. Flow cytometry analysis and Confocal laser scanning microscopy (CLSM) images verified the superior cellular uptake and intracellular trafficking behavior of HECP2k. In addition, HECP2k had excellent serum stability compared to PEI25k. The drug loading content and the drug loading efficiency of HECP2k@Dox were 13.83% and 41.49%, respectively. The Z-average sizes and zeta-potentials of HECP2k/siRNA

and HECP2k@Dox/siRNA were 153.7 nm, 14.67 mV, and 241.3 nm, 16.97 mV, respectively. In contrast to HeLa cells, HECP2k@Dox/siRNA nanocomplexes caused synergistically enhanced antitumor effect to HepG2 cells. HeLa cells were almost killed even at low concentration treatment of doxorubicin, but HepG2 cells showed above 60% of viability even at high concentration of Dox treated. However, when treated with HEPC2k@Dox/siRNA, the cell viability decreased by less than 50% in HepG2 cells. To estimate the synergistic effect of Bcl-2 siRNA/Dox co-delivery, a median effect analysis was conducted. By Annexin V staining analysis confirmed that HECP2k@Dox/siRNA caused cell death by inducing apoptosis. Consequently, HECP2k can be considered a promising Bcl-2 siRNA/Dox co-delivery carrier due to its high serum stability, great gene transfection efficiency, and improved antitumor effects.

Keyword : Gene/drug delivery systems, Hydroxyethyl cellulose, Polyethylenimine, Bcl-2 siRNA, Antitumor effect

Student Number : 2021-24540

Table of Contents

List of Tables

List of Figures

1. Introduction

A gene delivery system is a method of introducing new genes or suppressing over-expressed genes by transferring external genetic materials. An ideal gene delivery system requires high transfection efficiency, low cytotoxicity, and cell-specificity [1]. Gene carriers can be classified into viral and non-viral vectors. While viral vectors can bind with cell membranes and show high transfection efficiency, they possess problems such as evoking immune response and showing toxicity to host cells. Also, high cost and difficulties in mass production limit their pharmaceutical applications. In contrast, non-viral vectors are known to be safe compared to viral vectors. Despite lower transfection efficiency, non-viral vectors have the advantage of introducing the desired functions due to its ease of modification [2]. Therefore, non-viral vectors, including cationic polymers, liposomes and dendrimers, have been studied as gene carriers. The cationic polymers form complexes with anionic genes via electrostatic interaction and easy access negatively charged cell membranes [3].

For most conventional tumor chemotherapy, overcoming multi-drug resistance (MDR) remains as a challenge. MDR refers to the ability of cancer to resist treatment with drugs. Even if adequate doses of drugs are administered, chemotherapy can be hindered by MDR characteristics. MDR phenotype can be developed in result of prolonged chemotherapy or genetic alterations in tumor cells [4]. Although the mechanism of MDR is still unclear, drug efflux system of tumor cell and altered intracellular pathways to evade apoptosis are widely accepted mechanisms [5].

Recent studies reported that nanoparticles with chemotherapeutics could evade the

drug efflux pumps, increasing the intracellular drug concentration. However, the overall antitumor effect of delivered nanoparticles was insignificant since the increase in drug concentration did not cause a proportionate increase in cell death [6–8]. At a high drug concentration, silencing the genes in the anti-apoptosis pathway is essential to reverse MDR [4]. Therefore, the ideal design of carriers for drug and gene co-delivery is demanded to enhance the antitumor effect through synergism.

Hydroxyethyl cellulose (HEC) is the most abundant natural polymer, used for variety of applications for cosmetics or pharmaceutical use due to its biocompatibility. HEC also has great water solubility, thus does not require organic solvents in the synthesis process [9, 10]. In the biomaterial field, PEGylation is taken to increase serum stability [11–13]. When HEC is used as the primary material of gene carriers, the ethylene oxide oligomeric structure on the cellulose backbone may be considered to increase serum stability. Despite these advantages, there are few cases of developing HEC as efficient gene carriers. Notably, in our knowledge, there is no reported research to develop HEC as a gene/drug co-delivery system. This is supposed to be because appropriate chemistry for introducing the cationic moiety has not been developed. This study used simple chemistries such as periodate oxidation and reductive amination to introduce cationic moiety to HEC in the aqueous solution. It is expected to have excellent delivering efficiency with controlling the conjugation ratio of the cationic moiety. Polyethylenimine (PEI) is a cationic polymer under the pH conditions of the body and can form polyplexes with anionic genes. When PEI is used as a gene carrier, the endosomal escape occurs smoothly by the proton sponge effect [14, 15]. However, high molecular weight PEI shows cytotoxicity. Therefore, methods of reducing cytotoxicity have been reported

by conjugation with natural polymers or using low molecular weight PEI [16].

Bcl-2 proteins are especially overexpressed in tumor cells, inhibiting cell death and contributing to the abnormal growth of tumor [17, 18]. It is also known to be involved in the mechanism of drug resistance [19]. Therefore, researches have been conducted to suppress the expression of Bcl-2 proteins and apply them to cancer treatment [20–24].

In this study, PEI-conjugated HEC (HECP2k) was investigated for antitumor drug and Bcl-2 siRNA co-delivery system. PEI, of which molecular weight is 2000 kDa, was chosen to condense nucleic acids. PEI was also used for doxorubicin (Dox) loading by hydrogen bonding and physical embedding. Dox was used as an antitumor drug. For these reasons, HECP2k can be used as a novel gene/drug carrier for tumor treatment. When Dox/Bcl-2 siRNA loaded complexes (HECP2k@Dox/siRNA) are approached to tumor site, cellular uptake occurs in cancer cells in form of endosome. Through proton-sponge effect induced by PEI, Dox and Bcl-2 siRNA can be released to cytosol. Released Dox exhibits anticancer effect by disrupting DNA repair and generating free radicals, while Bcl-2 mRNA can be cleaved by RNA-induced silencing complex (RISC) composed of Bcl-2 siRNA. Downregulation of Bcl-2 protein results in apoptosis induction and enhancement of anticancer effect of Dox by reducing drug resistance (Figure 1). After synthesis of HECP2k, physicochemical properties were analyzed, the potential for gene delivery carrier was examined, and the potential for gene/drug co-delivery systems was examined by *in vitro* experiments.

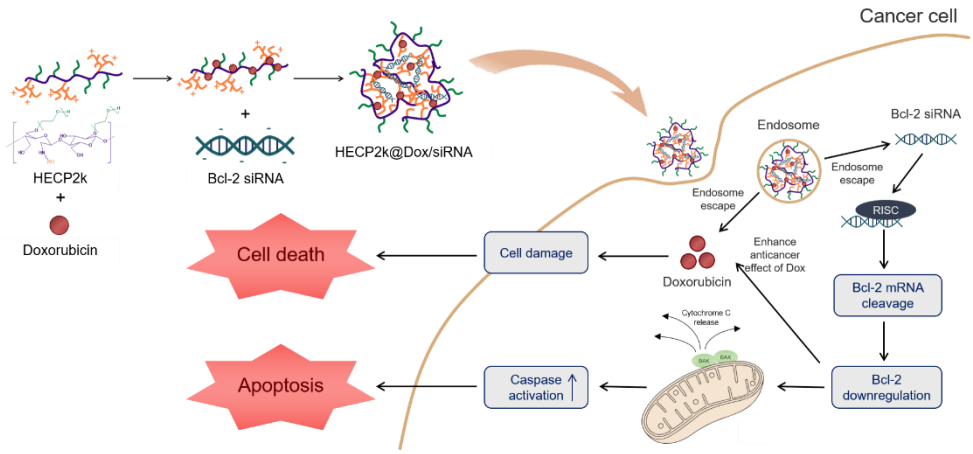

Figure 1. Schematic illustration showing formation and antitumor effect of the nanocomplex.

2. Literature Survey

2.1. Hydroxyethyl cellulose for gene/drug delivery systems

Polysaccharides are one of the candidates for efficient gene/drug delivery systems due to their high biocompatibility, biodegradability, chemically modifiable functional groups, and abundance [25]. Generally, cationic polymers such as PEI or other functionalities have been introduced to polysaccharides for gene delivery systems by chemical modifications of functional groups [26].

Hydroxyethyl cellulose (HEC) is one of the cellulose derivatives that hydroxyl groups on C2, C3, or C6 were substituted to hydroxyethyl groups. Synthesis of HEC is conducted by dissolution of cellulose in sodium hydroxide and reacting with ethylene oxide [27]. HEC has some advantages to be used in biomedical fields. Firstly, HEC is replenishable because its raw material is cellulose, the most abundant polysaccharide in nature. Second, HEC has great water solubility, which results in unnecessariness to use organic solvents. Also, the biocompatibility of HEC can act as a great advantage when applied to the biomedical fields such as cosmetics or pharmaceutics. The substituent of HEC is as same structure as poly(ethylene glycol) (PEG), commonly used for enhancing the plasma stability in biomedical fields [28]. Therefore, it can be reasonable to suppose that HEC can enhance the plasma stability as a main material for gene/drug delivery systems [29].

Despite these advantages, few cases have been developed as efficient gene carriers. Himmelein et al. developed HEC-based hydrogel containing cyclodextrin vesicles as 3D junctions [30]. Therapeutic agents could be loaded inside the vesicles, and

controlled release could be induced with the biocompatibility of the components. Ho et al. investigated HEC-based gel containing metronidazole-loaded lipid nanoparticles for buccal mucosal drug delivery [31]. Their hydrogel exhibited a sustained release pattern, and enhanced antimicrobial activity of treatment *in vitro*. Fayazpour et al. researched polyquaternium-4 (PQ-4) and polyquarternium-10 (PQ-10), the cationic hydroxyethyl cellulose materials commonly used in cosmetics and topical drug delivery devices, to use as a gene vector [29]. They aimed to characterize the properties of PQ-4/pDNA and PQ-10/pDNA nanoparticles, and noticed that the sugar monomers of PQ-4 and PQ-10 were substituted with PEG. However, PQ-4/pDNA and PQ-10/pDNA nanoparticles showed poor transfection efficiency, because of their neutrally charge surface and too strong binding of pDNA, respectively. Consequently, it can be worthwhile to develop a gene/drug delivery system with excellent transfection efficiency while taking advantages of HEC.

2.2. Cationic polymer for gene delivery

2.2.1. Viral vector and non-viral vector

Vectors for gene delivery can be classified into viral and non-viral vectors. By the various clinical trials of viral vectors for gene therapy, the limitations of viral vector were clearly revealed. Viral vectors have high transfection efficiency due to the virus's own gene transfer function. However, the safety issue related to the pathogenicity of the virus, transgenicity, and immune response have been raised consistently. As a result, researches on non-viral vectors that can overcome the limitations of the viral vector have been studied.

Cationic polymers or cationic lipids are widely used as non-viral vectors due to their ability to form complex with gene via electrostatic interaction. Despite non-viral vectors are advantageous in terms of safety and easy of modification, lower transfection efficiency than that of viral vector and cytotoxicity due to cationic charge were recognized as the limitations [32].

2.2.2. Necrosis process by cationic polymer

Cytotoxicity of the cationic polymer is a very important factor for evaluation of gene delivery systems. PEI is one of the most commonly used cationic polymer as gene carrier. However, high molecular weight PEI can exhibit significant cytotoxicity. The cytotoxicity of PEI reveals two types; cytotoxicity from the molecule itself and cytotoxicity from the polyplex [33]. Densely charged cationic polymers form clusters with various negatively charged protein in the body. The clusters access to cellular membrane, and destabilize the membrane. Eventually, clusters destruct the cellular membrane, and necrosis occurs. The cytotoxicity

from the polyplex is caused by dissociation of the internalized polyplex. Dissociated PEI interacts with various organelles and interfere the normal cell activities.

2.2.3. Research for overcoming the cytotoxicity of PEI

Many studies to overcome the cytotoxicity of PEI have been reported. Forrest et al. developed degradable PEI by crosslinking low molecular weight PEI (800 Da) with diacrylate crosslinker [34]. The molecular weight of their polymer was 14–30 kDa, and it has a similar structure and gene condensing ability to branched PEI. Also, the low cytotoxicity of the polymer was investigated. Cytotoxicity of the cationic polymer is also affected the structure of the polymer. Fischer et al. investigated the cytotoxicity of the globular (or branched) polymer such as PAMAM dendrimer and relatively flexible (or linear) polymer such as poly(L-lysine hydrobromide) (PLL) or linear PEI. By comparison of the cytotoxicity of branched and linear polymer, they investigated that more flexible molecules can access to cellular membrane easier than stiff molecules, thus contribute to the cytotoxicity [35].

Another strategy to decrease cytotoxicity is to conjugate the PEI with biocompatible natural polymers. Aldawsari et al. developed hyaluronic acid-based nanoparticles for pDNA delivery [36]. They synthesized PEI conjugated hyaluronic acid for gene carrier, and investigated the aspects that can be utilized for gene delivery vectors. This polymer exhibited negligible cytotoxicity in HeLa and A549 cells, and achieved the significant gene expression results. To sum up, there are such strategies including use of low molecular weight PEI, utilization of

stiff structure, or conjugation with natural polymers. Likewise, many researches to solve the problem of cytotoxicity have been conducted constituently

2.3. Bcl-2 siRNA for tumor therapy

2.3.1. RNA interference with siRNA for tumor therapy

RNA interference (RNAi) is a promising approach in treating variety of oncological, cardiovascular, and immunoregulational conditions. siRNA (small interfering RNA) is a type of nucleic acid downregulating the expression of a specific protein. In cytoplasm, siRNA binds to RNA-induced silencing complex (RISC). RISC recognizes the complementary mRNA and induces mRNA degradation. Degradation of target mRNA results in inhibition of protein synthesis [37]. siRNA is highly effective since activated outside the nucleus, also has an advantage of targeting ability due to complementary binding with specific sequence [38]. However, siRNA is characterized by low cellular uptake and are susceptible to nuclease-mediated degradation. Therefore, proper carriers are required for their protection and efficient delivery [39].

2.3.2. Role of Bcl-2 protein in tumor

Bcl-2 was the first anti-death gene discovered. Various Bcl-2 family proteins regulates apoptosis, necrosis, and autophagy. Bcl-2 protein participates in the mitochondrial apoptosis pathway in normal cells, and function to suppress cell death. When given stimuli, BH3-only protein is activated. The activated BH3-only protein oligomerizes BAK/BAX at the mitochondrial membrane, which causes permeability of mitochondrial membrane. After that, Cytochrome C is released from the mitochondria, which activates caspase 9, leads to apoptosis by the downstream pathway. Bcl-2 protein functions as antagonist to BH3 protein. Bcl-2 protein binds to BAK/BAX instead of BH3, which induces dysfunction of

mitochondria [40]. Bcl-2 proteins are overexpressed in tumor, which results in cell death and abnormal growth of tumor [19] (Figure 2).

2.3.3. Synergistic antitumor effect by co-delivery of antitumor drugs and Bcl-2 siRNA

Bcl-2 protein also known to be involved in drug resistance of tumor. Regardless of the primary mechanisms of pharmacological actions, whether DNA breaks, microtubule depolymerization, or hormone receptor inhibition, most of the conventional anticancer drugs appear to depend on Bcl-2 protein [41, 42]. Many studies for tumor therapy with downregulation of Bcl-2 expression have been reported [20–25, 43–44]. Among them, there were researches that expected synergistic effects by co-delivery of anticancer drugs and Bcl-2 siRNA. Doxorubicin, a conventional anticancer drug, inhibits the catalytic action of topoisomerase II, forms free radicals, and binds to DNA, exhibiting anticancer effects. Ye et al. developed galactose-conjugated methacrylate-based polymer for Dox and Bcl-2 siRNA co-delivery [43]. Galactose on their polymer enabled active targeting, and co-delivery of anticancer drug Dox and Bcl-2 siRNA worked synergistically against tumor growth *in vivo*. Chen et al., investigated co-delivery of Dox and Bcl-2 siRNA by mesoporous silica nanoparticles (MSNs) [44]. They synthesized the MCM-41 type of MSNs using a surfactant-templated, base-catalyzed condensation method to delivery Dox and siRNA to multidrug resistant A2780/AD human ovarian cancer cells. Bcl-2 expression was effectively silenced and efficacy of chemotherapy was also enhanced. Therefore, it is thought to have potential to develop a efficient co-delivery system for synergistic anticancer action

of anticancer drugs and Bcl-siRNA.

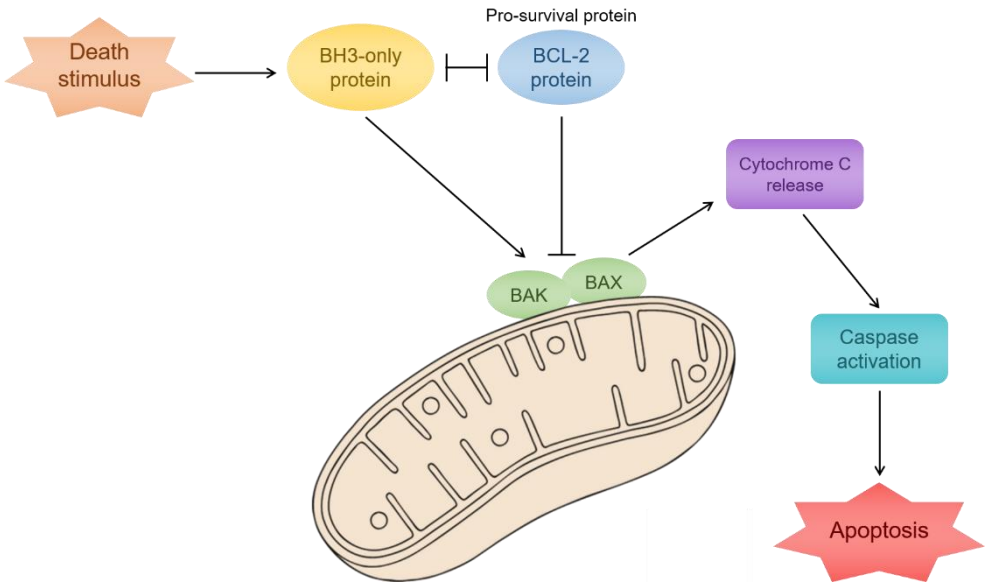

Figure 2. Schematic diagram showing a apoptosis induction of Bcl-2 protein.

3. Materials and Methods

3.1. Materials

Hydroxyethyl cellulose (HEC), branched polyethylenimine (PEI25k, 25kDa), agarose, gel loading solution, ethidium bromide (EtBr), dimethyl sulfoxide (DMSO), MicroBCA™ protein assay kit, 4',6-diamidino-2-phenylindole (DAPI), and triethylamine (TEA) were purchased from Sigma-Aldrich (USA). Branched polyethylenimine (PEI2k, 2000 Da) was purchased from Polyscience (USA). Sodium metaperiodate was purchased from Alfa-aesar (USA). Sodium tetrahydroborate and HPLC water were purchased from Duksan (Korea). Dialysis membrane (MWCO 3.5 kDa) was purchased from SpectrumLABS (USA). Formic acid was purchased from Merck (Germany). Triazolyl blue tetrazolium bromide (MTT) was purchased from GoldBio (USA). pDNA (pCN-Luci) was amplified by using Dyne DH5α Chemically Competent *E.coli* ver.2 (DYNEBIO, Korea) and purified by using NucleoBond® Xtra Maxi (Macherey-Nagle, Germany). Dulbecco's Modified Eagle Medium (DMEM) and Dulbecco's phosphate buffered saline (DPBS) were purchased from Cytiva (Korea). DMEM GlutaMAX™ (GMX), fetal bovine serum (FBS), penicillin streptomycin (P/S) and trypsin-EDTA were purchased from Gibco (USA). Luciferase assay system and reporter lysis buffer were purchased from Promega (USA). YOYO-1 iodide and Lysotracker™ Red DND-99 were purchased from Invitrogen (USA). Doxorubicin hydrochloride (Dox·HCl) was purchased from Cayman Chemical (USA). Alexa Fluor® 488 Annexin V/Dead cell apoptosis kit was purchased from Life Technology. Bcl-2 siRNA (5'-

GUGAAGUCAACAUGCCUGC-3’ (sense), 5’-GCAGGCAUGUUGACUUCAC-3’ (anti-sense)) was purchased from Bioneer (Korea).

3.2. Methods

3.2.1. Synthesis of HECP2k (Polyethylenimine 2000Da-conjugated Hydroxyethyl cellulose)

Prior to HECP2k synthesis, HEC oxidation was proceeded. HEC and sodium metaperiodate was dissolved in water solution respectively. Then, sodium metaperiodate ($NaIO_4$) solution with one molar equivalent of the sugar units was added to HEC solution with continuous stirring. After 2 h of reaction under 25 ℃ in the dark, the solution was dialyzed against ultra-pure water for 48 h using dialysis membrane (MWCO 3.5 kDa). The product, oxidized-HEC (OxHEC) was obtained after lyophilization.

HECP2k was synthesized by reductive amination of OxHEC and PEI2k. To synthesize HECP2k, OxHEC was dissolved in water solution. Then various amounts of PEI2k solution (HEC:PEI2k = 1:1, 1:5, or 1:10 w/w, respectively) were prepared in reaction bottles and OxHEC solutions were added to the bottles with continuous stirring. After 24 h of reaction under 25 ℃ in the dark, excessive sodium tetrahydroborate ($NaBH_4$) was added to the reaction bottles with continuous stirring. After 24 h of reaction 25 ℃ in the dark, the solutions were dialyzed against ultra-pure water for 72 h using dialysis membrane (MWCO 3.5 kDa). The products, HECP2k 1X, 5X, or 10X were obtained after lyophilization. The synthesis scheme of HECP2k was shown in Figure 3.

3.2.2. Characterization of HECP2k

3.2.2.1. Structural analysis with ^{1}H NMR and primary amine quantification

The synthesis of the polymers was confirmed by ^{1}H NMR (600MHz, AVANCE 600, Brucker, Germany). D_2O was used as the solvent. Each sample was prepared at a concentration of 10 mg/mL.

The primary amine (1° amine) quantification of HECP2k was performed by using Fluorescamine. Calibration curve was drawn with PEI2k as a standard. The primary contents of the PEI2k (molar amounts of 1°:2°:3° amine = 40:36:24) was referred to the manufacturer's site. HECP2k samples were diluted with PBS buffer into 10 μg/mL. 75 μL of sample solutions and 25 μL of fluorescamine solution (3 mg/mL, DMSO) were reacted for 15 min at 25 ℃. The fluorescence was measured at Ex/Em=380/470 nm with a microplate reader (Synergy H1, BioTek, USA). After the measurements, the molar amounts of primary amine per 1 g of HECP2k were calculated for each sample, and compared with ^{1}H NMR results.

3.2.2.2. Molecular weight measurements with GPC

The molecular weights of the polymers were measured by Gel Permeation Chromatography (GPC, YL-9100 HPLC System, Youngin Chromass, Korea). Each sample was prepared at a concentration of 10 mg/mL. 1% formic acid was used as the solvent. Poly (ethylene glycol)s with various molecular weights were used as standards for analysis. The assay was run on Ultrahydrogel 250 column (Waters, USA) at 0.6 mL/min of flow rate.

3.2.2.3. Structural analysis with ^{13}C NMR and FT-IR

The synthesis of the polymer was confirmed by ^{13}C NMR (600MHz, AVANCE 600, Brucker, Germany). D_2O was used as the solvent. The sample was prepared at a concentration of 50 mg/mL.

The synthesis of the polymers was confirmed by FT-IR (Nicolet iS5 FTIR spectrometer, Thermo scientific, US). ATR (Attenuated Total Reflectance) spectroscopy (Nicolet 6700, Thermo Scientific, USA) was used. The measurements were performed in the wavenumber range of 4000–650 cm^{-1} with 32 scans.

3.2.3. Characterization of HECP2k/pDNA polyplex

3.2.3.1. pDNA condensing ability with agarose gel electrophoresis

pDNA condensing ability of HECP2k was examined by agarose gel electrophoresis. HECP2k/pDNA polyplexes were prepared in Hepes buffer (pH 7.4) at various weight ratios ranging from 0.1 to 0.9 for HECP2k 1X, and from 0.1 to 0.5 for HECP2k 5X and 10X. Agarose gel (0.7% w/v) containing EtBr solution (0.5 μg/mL) was prepared in TAE (Tris-Acetate-EDTA) buffer. After 30 min of incubation at room temperature, the samples were electrophoresed at 80 V for 12 min using Mupid-2plus® (OPTIMA, Japan). The pDNA bands were visualized with GelDoc™ XRS+ gel documentation system (BIO-RAD, USA).

3.2.3.2. Average size and zeta-potential measurements with DLS

Average sizes and zeta-potential values of the polyplexes were measured by using Zetasizer Nano ZS (Malvern Instruments, UK). The polyplex solutions were prepared in ultra-pure water at various weight ratios ranging from 0.1 to 30. The final volume of the solutions was 1 mL. After 30 min of incubation at room temperature, the measurements were performed 3 times

3.2.4. *In vitro* assay of HECP2k and HECP2k/pDNA polyplex

3.2.4.1. Cell culture

Human cervical adenocarcinoma cells (HeLa) and human hepatocellular carcinoma cells (HepG2) were used for *in vitro* experiments. Cell culture was proceeded in cell medium containing 10% of FBS and 1% of penicillin/streptomycin (P/S). DMEM GlutaMAX™ and DMEM were used as medium for HeLa cells and HepG2 cells respectively. 37 ℃ and 5% of CO_2 condition was maintained for cell culture.

3.2.4.2. Cell metabolic activity with MTT assay

The cytotoxicity of HECP2k was estimated with MTT assay. The cells (HeLa and HepG2) were seeded on a 96-well cell culture plate at a density of 1×10^4 cells/well in 100 μL of medium containing 10% FBS and 1% P/S. As the cells achieved 70–80% confluency after 24 h of incubation, the cells were treated with HECP2k solutions (serum-free medium) with various concentrations from 0 μg/mL to 100 μg/mL for 4 h. PEI25k was used as a control group. Then, the medium was exchanged with fresh medium containing 10% FBS. After 24 h of incubation, 25 μL of MTT solution (2 mg/mL) was added to each well and further incubated for 2 h. After the incubation, the medium was removed and 150 μL of DMSO was added to each well to dissolve formazan crystal formed by cell metabolism. The absorbance was measured at 570 nm by using a microplate reader (Synergy H1, BioTek, USA). The results were presented as relative cell viability (RCV, %) through calculation of the percentage values relative to untreated control group.

3.2.4.3. Gene transfection efficiency with luciferase transgene expression assay

The transfection efficiency of HECP2k was estimated with luciferase transgene expression assay. The cells (HeLa) were seeded on a 24-well cell culture plate at a density of 5×10^4 cells/well in 500 μL of medium containing 10% FBS and 1% P/S, and incubated for 24 h as the cells achieved 70–80% confluency. The HECP2k/pDNA polyplex solutions with various weight ratios were prepared in ultra-pure water for 50 μL each. Prior to treatment, medium was exchanged to 450 μL of fresh medium (both of serum-free medium and serum containing medium). Then, the cells were treated with HECP2k/pDNA polyplex solutions (0.5 μg of pDNA/well) with various weight ratios for 4 h. PEI25k/pDNA polyplex (weight ratio = 1) was used as a positive control group. After the incubation, the medium was exchanged with fresh medium containing 10% FBS. After 48 h of incubation, each medium was aspirated, the cells were rinsed with DPBS and lysed with 120 μL of Reporter lysis buffer. The cell lysates were centrifuged (14000 RPM, 10 min, 4 ℃), and the supernatants were collected. 20 μL each of the supernatant was added to a white 96-well plate, and 100 μL of the luciferase assay buffer were dispensed to each well. The luminescence was measured by using a microplate reader (Synergy H1, BioTek, USA). To quantify the amounts of protein in the supernatant, MicroBCA™ protein assay kit was used. 130 μL of ultra-pure water, 150 μL of BCA reagent, and 20 μL of the supernatant were dispensed to 96-well plate. After 2 h of incubation at 37 ℃, the absorbance was measured at 562 nm by using a microplate reader. The results were presented in terms of relative luminescence unit per unit mg of cellular protein (RLU/mg protein).

3.2.4.4. Cellular uptake measurement with Flow cytometry

To estimate cellular uptake of the HECP2k/pDNA polyplex, flow cytometry was used. Cells (HeLa) were seeded on a 6-well cell culture plate at a density of 2×10^5 cells/well in 2 mL of medium containing 10% FBS and 1% P/S, and incubated for 24 h as the cells achieved 70–80% confluency. pDNA labeled with YOYO-1 iodide (1 dye molecule per 50 base pairs of nucleotides) was prepared. The HECP2k/pDNA polyplex solutions with various weight ratio were prepared. Then, the cells were treated with polyplex solutions (1 μg of pDNA/well) for 4 h. After 4 h, the medium was aspirated, and the cells were rinsed with ice-cold DPBS. Trypan blue solution (1 mg/mL) was treated to quench unnecessary fluorescence at outer cell membrane. The cells were rinsed with DPBS twice. After 2 min of trypsinization, the detached cells were re-suspended in DPBS. The cellular uptake of fluorescence-labeled polyplexes and the mean fluorescence were examined by using BD Accuri C6 flow cytometer at a minimum of 1×10^4 cells gated per sample. The analysis was performed by using BD Accuri C6 software.

3.2.4.5. Intracellular trafficking visualization with CLSM

Cells (HeLa) were seeded on a confocal dish at a density of 3×10^5 cells/dish in 3 mL of medium containing 10% FBS and 1% P/S, and incubated for 24 h as the cells achieved 70–80% confluency. pDNA labeled with YOYO-1 iodide (1 dye molecule per 50 base pairs of nucleotides) was prepared. The HECP2k/pDNA polyplex solutions with optimal weight ratio (weight ratio = 50) were prepared in ultra-pure water for 300 μL each. Prior to treatment, medium was exchanged to

2700 μL of fresh medium. Then, the cells were treated with polyplex solutions (1.5 μg of pDNA/dish) for 4 h. PEI25k/pDNA polyplex (weight ratio = 1) was used as a control group. After 4 h of incubation, the medium was exchanged with fresh medium containing 10% FBS, and incubated for 0 h, 2 h, or 4 h. Then, acidic organelles were stained by Lysotracker™ Red DND-99 solution (100 nM), and the cells were fixed with 4% para-formaldehyde. Nuclei were labeled with DAPI solution (0.125 μg/mL). Cells were rinsed sufficiently. Visualization proceeded with Confocal Laser Scanning Microscope (SP8 X STED, Leica, Germany), and the images were processed with LAS X software.

3.2.4.6. Serum stability test

To estimate serum tolerance of HECP2k polyplex, cells were seeded on a 24-well cell culture plate at a density of 5×10^4 cells/well and incubated for 24 h until they achieved 70–80% confluency. Before transfection, medium of each well was exchanged with fresh medium containing various FBS concentrations; 10, 30, 50%, respectively. Then polyplex solutions (0.5 μg of pDNA/well) were treated to each well with optimal ratio (weight ratio = 50) for 4 h. PEI25k was used as a control. After 4 h of treatment, the medium was exchanged with fresh medium containing 10% FBS, the cells were further incubated for 48 h. Then, each medium was aspirated, the cells were rinsed with DPBS and lysed with 120 μL of Reporter lysis buffer. The cell lysates were centrifuged (14000 RPM, 10 min, 4 °C), and collected the supernatants. 20 μL each of the supernatant was added to a white 96-well plate, and 100 μL of the luciferase assay buffer were dispensed to each well. The luminescence was measured by using a microplate reader (Synergy H1, BioTek,

USA). To quantify the amounts of protein in the supernatant, MicroBCA™ protein assay kit was used. 130 μL of ultra-pure water, 150 μL of BCA reagent, and 20 μL of the supernatant were dispensed to 96-well plate. After 2 h of incubation at 37 ℃, the absorbance was measured at 562 nm by using microplate reader. The results were presented in terms of relative luminescence unit per unit mg of cellular protein (RLU/mg protein).

3.2.5. Antitumor effect of HECP2k@Dox/siRNA

3.2.5.1. Doxorubicin loading and siRNA complexation

Dox·HCl was dissolved in DMSO at a final concentration of 5 mg/mL. 2 molar excess of Triethylamine (TEA) was added to Dox·HCl solution with continuous stirring for 24 h. After desalting, Dox solution was added dropwise to HECP2k solution (5 mg/mL, DMSO:DIW=1:9) with continuous stirring for 90 min. Then, all the product was added dropwise to 10 mL of ultra-pure water with continuous stirring for 24 h, and dialyzed against ultra-pure water for 6 h using dialysis membrane (MWCO 2 kDa) for 6 h. The product, HECP2k@Dox was obtained after lyophilization.

The absorbance of HECP2k@Dox solution (DMSO:DIW=1:9) was measured at 480 nm by using microplate reader (Synergy H1, BioTek, USA). Loaded Dox amount was determined according to the prepared calibration curve of Dox solution (DMSO:DIW=1:9). Drug loading content (DLC) and drug loading efficiency (DLE) were calculated as following formula.

$$\text{DLC}\ (\%) = \frac{Weight\ of\ loaded\ Dox}{Weight\ of\ HEPC2k} \times 100$$

$$\text{DLE}\ (\%) = \frac{Weight\ of\ Loaded\ Dox}{Weight\ of\ total\ Dox\ for\ loading} \times 100$$

Bcl-2 siRNA complexation was conducted to prepare HECP2k/siRNA polyplexes and HECP2k@Dox/siRNA complexes. HECP2k and HECP2k@Dox were mixed with Bcl-2 siRNA in ultra-pure water at a weight ratio of 50 (w/w). The complexes were incubated at 25 ℃ for 30 min.

3.2.5.2. Average size and zeta-potential of polyplex

Average size and zeta-potential value of HECP2k@Dox/siRNA nano-complex were measured by using Zetasizer Nano ZS (Malvern Instruments, UK). The complex solution was prepared in ultra-pure water at an optimal weight ratio (weight ratio = 50). The final volume of the solutions was 1 mL. After 30 min of incubation at room temperature, the measurements were performed 3 times

3.2.5.3. Antitumor effect analysis with MTT assay

The antitumor effect of the HECP2k@Dox/siRNA was estimated by MTT assay. The cells (HepG2) were seeded on a 96-well cell culture plate at a density of 1×10^4 cells/well in 100 μL of medium containing 10% FBS and 1% P/S. As the cells achieved 70–80% confluency after 24 h of incubation, the cells were treated for 4 h in serum-free medium with Dox (Dox·HCl), siRNA, PEI25k/siRNA, HECP2k/siRNA, HECP2k@Dox, HECP2k@Dox/siRNA, respectively. Concentration of siRNA and Dox were adjusted 3 groups; low (0.5 μg/mL of siRNA or 3.7 μg/mL of Dox), mid (1 μg/mL of siRNA or 7.4 μg/mL of Dox), and high (2 μg/mL of siRNA or 14.8 μg/mL of Dox). DLC value and the optimal weight ratio of polymer/pDNA (= 50 for HECP2k and = 1 for PEI25k) was considered to adjust the concentrations of Dox and siRNA. Then, the medium was exchanged with fresh medium containing 10% FBS. After 24 h of incubation, 25 μL of MTT solution (2 mg/mL) was added to each well and further incubated for 2 h. After the incubation, the medium was removed and 150 μL of DMSO was added to each well to dissolve formazan crystal formed by cell metabolism. The absorbance was measured at 570 nm by using a microplate reader (Synergy H1,

BioTek, USA). The results were presented as relative cell viability (RCV, %) through calculation of the percentage values relative to untreated control group. Statistical analysis was proceeded through one-way ANOVA and Bonferroni post-hoc test. Statistical significance was presented as follows. ($P<0.05$ *, $P<0.01$ **, $P<0.001$ ***)

3.2.5.4. Apoptosis induction test with Annexin V staining

The apoptosis induction was investigated by Annexing V staining using Alexa Fluor® 488 Annexin V/Dead cell apoptosis kit. Cells (HepG2) were seeded on a 6-well cell culture plate at a density of 2×10^5 cells/well in 2 mL of medium containing 10% FBS and 1% P/S, and incubated for 24 h as the cells achieved 70–80% confluency. Then, the cells were treated for 4 h in serum-free medium with HECP2k@Dox/siRNA. Concentration of siRNA and Dox were adjusted to 2 μg/mL and 14.8 μg/mL, respectively. The medium was exchanged with fresh medium containing 10% FBS. After 24 h of incubation, the cells were rinsed with iced DPBS twice. After 2 min of trypsinization, the detached cells were re-suspended in 500 μL of DPBS. To label the pro-apoptotic cell, Alexa Fluor® 488 solution was used. 5 μL of Alexa Fluor 488® solution and 10 μL of Propidium iodide (PI) solution were added into the cell suspension. After 15 min of incubation in 25 ℃ dark condition, the cells were sorted by BD Accuri C6 flow cytometer. The analysis was performed by using BD Accuri C6 software.

4. Results and Discussion

4.1. Synthesis and Characterization of HECP2k

4.1.1. Synthesis of HECP2k

Prior to synthesize HECP2k, HEC was oxidized by periodate oxidation with sodium metaperiodate in aqueous solution. Aldehyde groups were introduced by cleaving the vicinal diols in anhydroglucose units of HEC. After obtaining oxidized HEC (OxHEC), PEI was conjugated with various weight ratio (OxHEC:PEI) of 1:1, 1:5, and 1:10 by Schiff base formation, and reduced by sodium tetrahydroborate. PEI2k was almost 100% removed by dialysis with dialysis membrane (MWCO 3.5 kDa). Therefore, HECP2k with three different feed ratios of 1:1, 1:5, and 1:10 was obtained and named HECP2k 1X, 5X, and 10X, respectively (Figure 3).

4.1.2. Structural analysis with ^{1}H NMR and primary amine quantification

Structural analysis of HECP2k with three different feed ratios of 1X, 5X, and 10X were performed by ^{1}H NMR (Figure 4). Proton peaks of HEC and PEI2k were observed at δ 3.1–4.7 and δ 2.4–3.0, respectively. The NMR spectra of HECP2k 1X, 5X, and 10X confirmed that conjugation between HEC and PEI was successfully performed. According to manufacturer, the viscosity of HEC is ~145 mPa·s, in 1% H_2O (20℃) and the average molecular weight of HEC is ~250,000

Da. Assuming that the total molar of substitution is 2.5 and comparing all the proton peaks of HEC and PEI, it was calculated that one molecule of PEI2k was grafted to every 18.4, 5.8, and 2.4 sugar molecules of HECP2k 1X, 5X, and 10X, respectively. Converting this value into the number of moles of primary amines per unit mass of the polymer, 2.7 mmole/g, 5.2 mmole/g, and 7.0 mmole/g of primary amines were present in HECP2k 1X, 5X, and 10X, respectively (Table 1).

Primary amine quantification with using fluorescamine was further performed to analysis the chemical structure of HECP2k. The calibration curve was calculated by using PEI2k as a standard (Figure 5). Fluorescamine reacted with primary amines in HECP2k for 15 min in 25℃ dark condition, and the fluorescence was measured at the wavelength of Ex/Em=380/470 nm. The fraction of primary amine in total amines was assumed to 40% by the information of manufacturer. As a result, the molar amount of primary amine per unit mass of the polymer was calculated to 1.48 mmole/g, 2.13 mmole/g, and 3.86 mmole/g for HECP2k 1X, 5X, and 10X, respectively (Table 1). The tendency of amount of primary amine was correlated with the previous proton NMR result. The discordance between amounts of primary amine by fluorescamine and that of ^{1}H NMR, would be derived from the unreacted primary amine with fluorescamine by the steric hinderance.

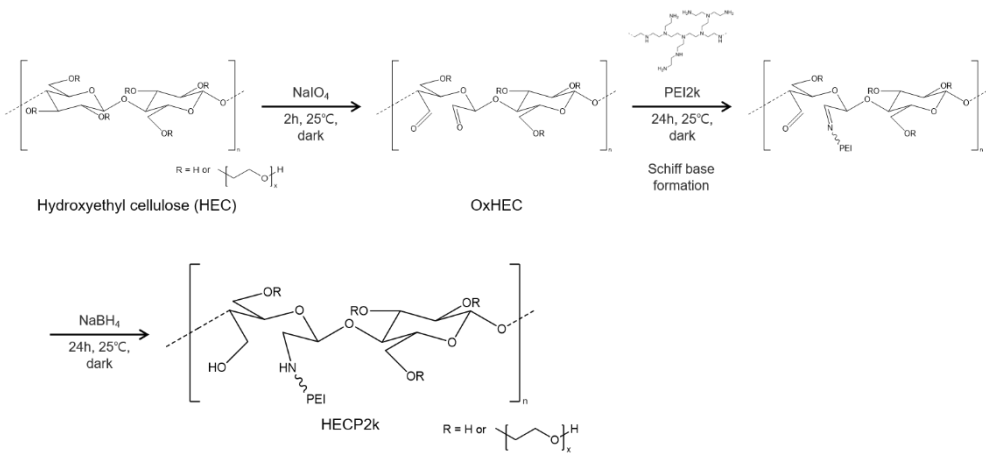

Figure 3. Synthesis scheme of HECP2k.

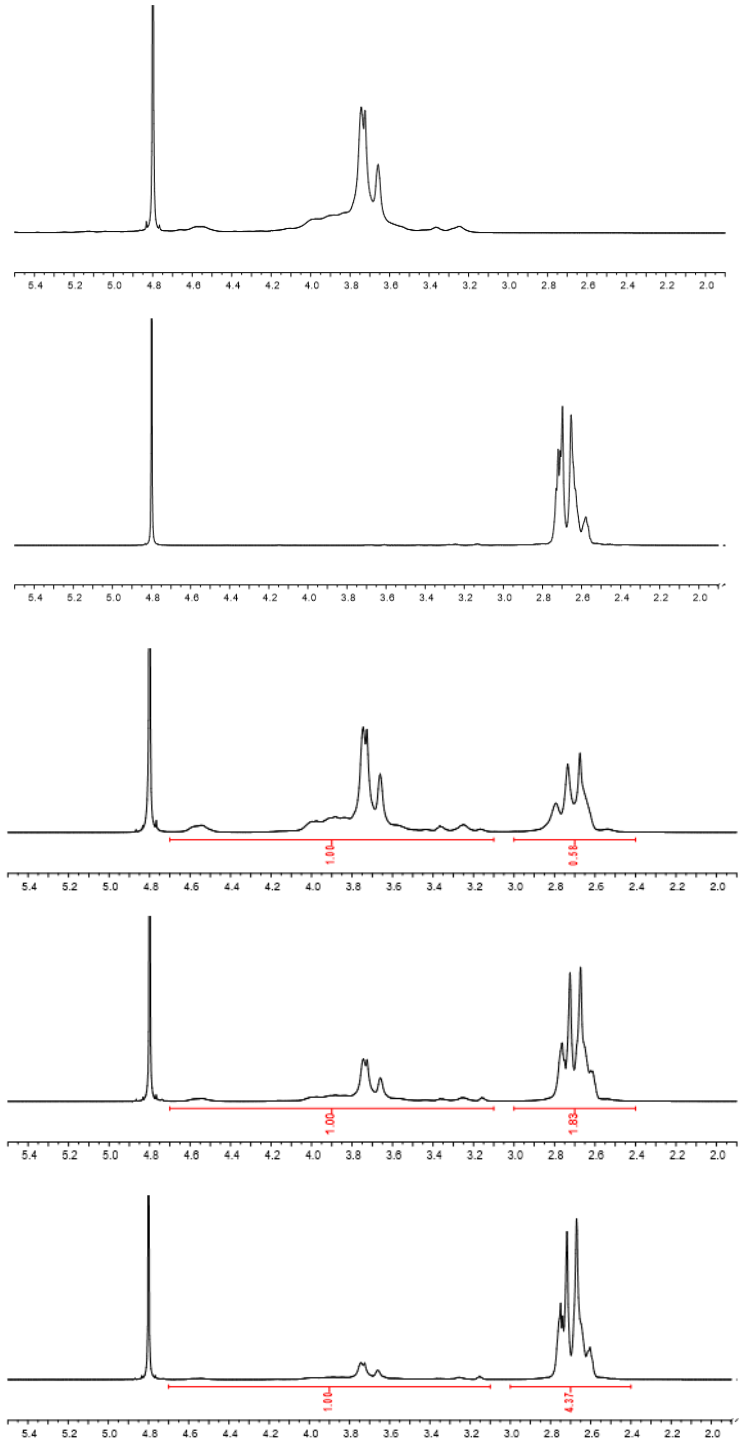

Figure 4. ^{1}H NMR spectra of (A) HEC, (B) PEI2k, (C) HECP2k 1X, (D) HECP2k 5X, (E) HECP2k 10X.

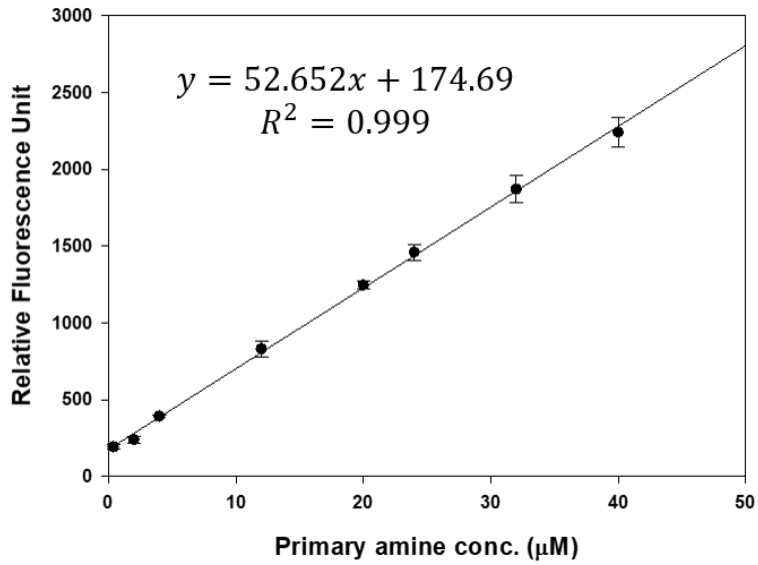

Figure 5. Calibration curve for primary amine quantification (PEI2k standard).

Table 1. Molar amounts of primary amine per unit mass of polymers.

Sample	1° amine (mmol/g) (^{1}H NMR)	1° amine (mmol/g) (quantification by fluorescamine)
HECP2k 1X	2.7	1.48
HECP2k 5X	5.2	2.13
HECP2k 10X	7.0	3.86

4.1.3. Molecular weight measurements with GPC

Molecular weight of HECP2k was measured by using GPC (Figure 6, Table 2). Identifying the absolute molecular weight by using GPC is difficult, because retention time could be affected by other factors such as column interaction, hydrophilicity, and 3-dimensional structure of the polymer [45]. Nevertheless, GPC is widely performed to compare the relative molecular weight of natural or synthetic polymers having similar physiochemical properties. The analysis was performed for comparing each relative molecular weight of HECP2k 1X, 5X, and 10X, and verifying purification.

Each chromatogram of HECP2k 1X, 5X, and 10X was exhibited as a single peak. This demonstrated that synthesis and dialysis were performed well. The weight average molecular weight (Mw) and PDI of OxHEC were 35.63 kDa and 5.89, respectively. Mw and PDI of PEI2k were 4.61 kDa and 2.36, respectively. For HECP2k 1X, 5X, and 10X, Mw was 13.92 kDa, 9.38 kDa, and 7.27 kDa, respectively, and PDI was 2.37, 2.36, and 2.25, respectively. The reason why the molecular weights of HECP2k 1X, 5X, and 10X were measured lower than OxHEC was thought to be due to the variation of the interaction with column after conjugation of PEI, as previously mentioned. Interestingly, the Mw decreased as the conjugation ratio of PEI increased. This could be explained by appropriate stoichiometric balance between two different multi-functional polymers in HECP2k 1X. Whereas in HECP2k 5X and 10X, excess amount of PEI disrupted stoichiometric balance which caused decrease in Mw.

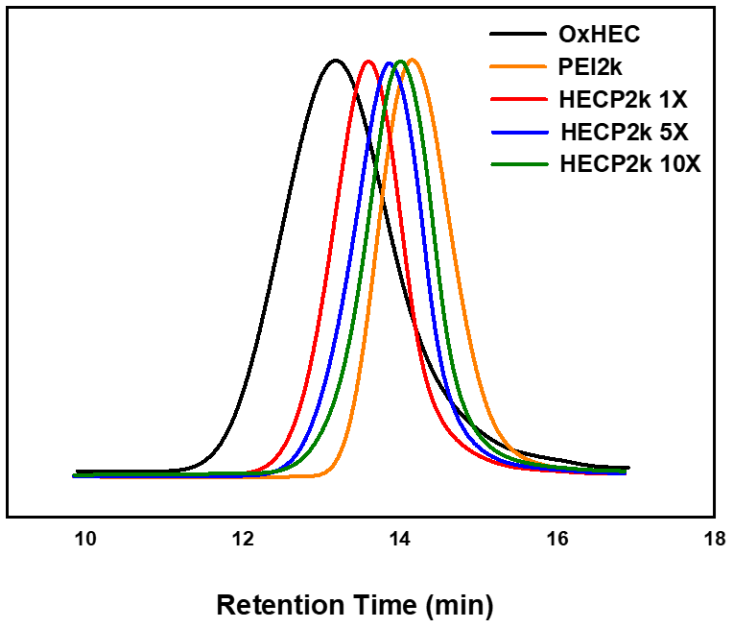

Figure 6. GPC chromatograms of OxHEC, PEI2k, HECP2k 1X, HECP2k 5X, HECP2k 10X.

Table 2. Molecular weight of OxHEC, PEI2k, HECP2k 1X, HECP2k 5X, HECP2k 10X by GPC (PEG standard).

Sample	$M_{n\ (GPC,\ kDa)}$	$M_{w\ (GPC,\ kDa)}$	$PDI_{(GPC)}$	$RT_{(min)}$
OxHEC	6.05	35.63	5.89	13.21
PEI2k	1.95	4.61	2.36	14.25
HECP2k 1X	5.88	13.92	2.37	13.70
HECP2k 5X	3.97	9.38	2.36	13.95
HECP2k 10X	3.23	7.27	2.25	14.09

4.1.4. Structural analysis with ^{13}C NMR and FT-IR

Additional structural analyses for optimized HECP2k 10X were conducted with ^{13}C NMR (Figure 7) and FT-IR (Figure 8). ^{13}C NMR spectra of HECP2k 10X showed broad carbon peaks of cellulose backbone at δ 68–103. The peaks of ethylene oxide were observed at δ 60–62. Also, carbon peaks of PEI were observed at δ 37–58. Each peak was well exhibited by the ^{13}C NMR spectra.

Aldehyde formation by periodate oxidation was identified by comparing the FT-IR spectra of HEC and OxHEC. C=O peak (1740–1720 cm^{-1}) was absent in HEC spectra, but unprecedented peak was observed in OxHEC peak. Also, N-H and C-N peaks were observed in both PEI2k and HECP2k spectra. Notably, C=O peak disappeared in HECP2k spectra, which means aldehyde groups were absent in HECP2k due to the successful Schiff base formation conducted.

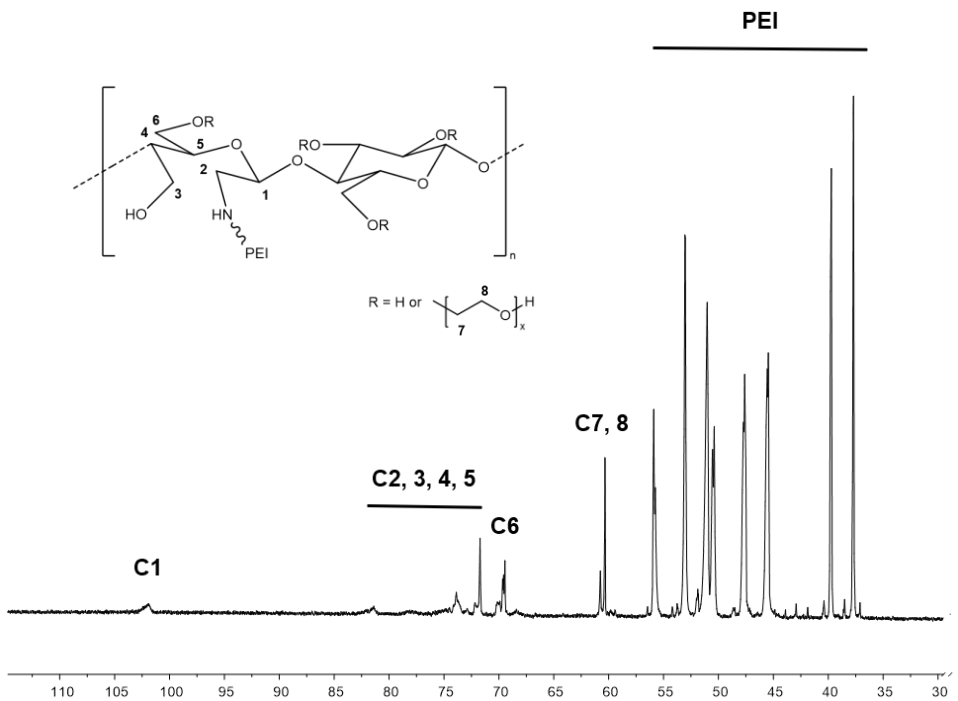

Figure 7. ^{13}C NMR spectra of HECP2k 10X.

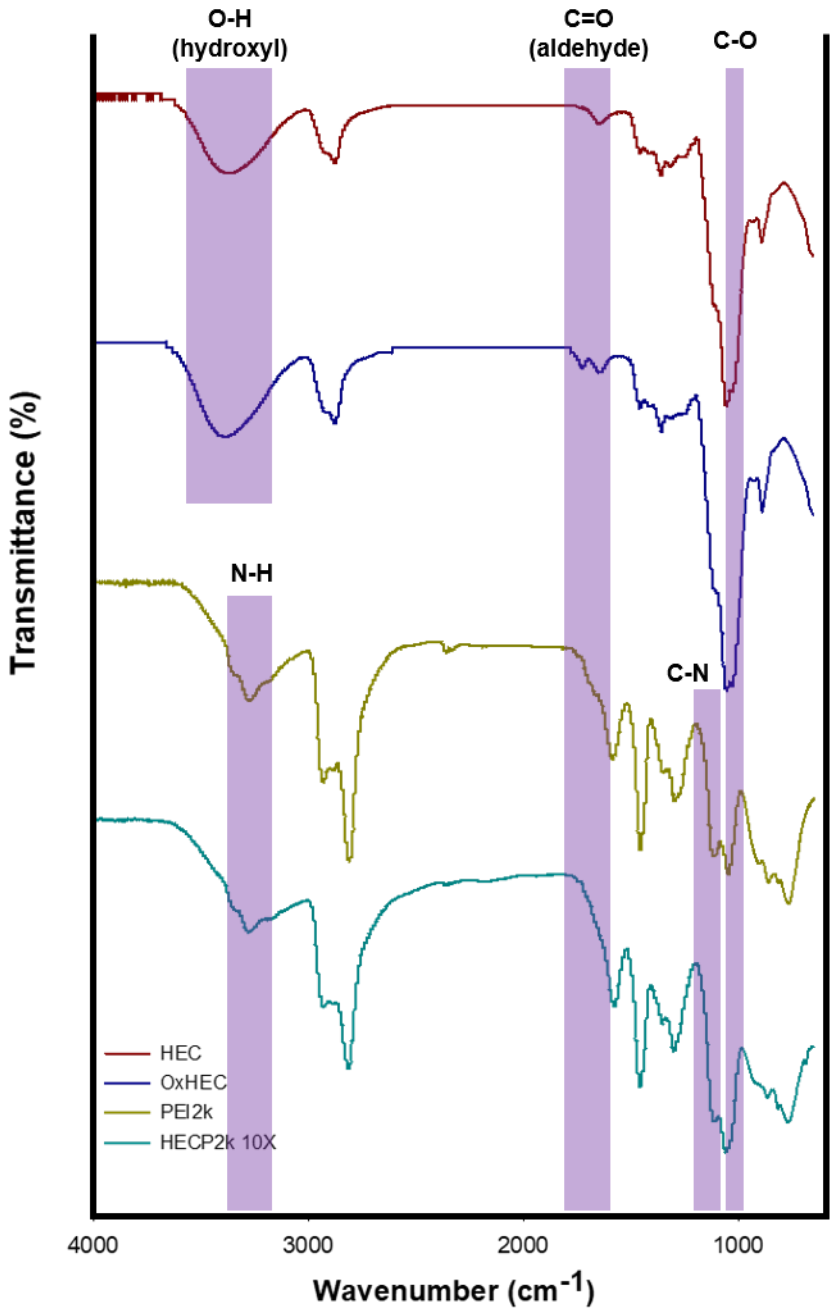

Figure 8. FT-IR spectra of HEC, OxHEC, PEI2k, HECP2k 10X.

4.2. Characterization of HECP2k/pDNA polyplex

4.2.1. pDNA condensing ability with agarose gel electrophoresis

Agarose gel electrophoresis was conducted to examine the pDNA condensing ability of HECP2k (Figure 9). HECP2k, a cationic polymer, can form polyplexes with negatively charged pDNA by electrostatic interaction. HECP2k 10X could condense pDNA completely at a weight ratio of 0.3, but HECP2k 1X and 5X could condense pDNA at a higher weight ratio of 0.9 and 0.5, respectively. This result demonstrated that the pDNA condensing ability of HECP2k increases as the conjugation ratio (or feed ratio) of PEI/HEC increases.

4.2.2. Average size and zeta-potential measurements

The transfection efficiency of gene carriers can be affected by particle size and surface charge. If the size of the polyplex is too large or too small, the polyplex could be removed by the liver, kidney, or reticuloendothelial systems. Generally, 100 nm to 200 nm is known as suitable size for endocytosis. Also, a cationic surface charge is advantageous due to the easy access to the cellular membrane. However, the excessive cationic charge can cause cell death by necrosis.

Average particle size and zeta-potential value of HECP2k/pDNA polyplexes were measured at various weight ratios of 0.3, 0.5, 1, 5, 10, 20 and 30 by Zeta-sizer (Figure 10). Z-average sizes of all HECP2k/pDNA polyplexes were found to be above 100 nm and below 300 nm at higher weight ratios than 1. The drastic increased size was observed at a weight ratio of 0.5 in HECP2k 10X. It was thought to be due to the aggregation of the neutrally charged particles. As a result

of zeta-potential measurement, HECP2k 1X was found to be negatively charged at weight ratios of 0.3 and 0.5, roughly neutral at a weight ratio of 1, and retain a positive charge of approximately 20–30 mV at weight ratio above 5. HECP2k 5X and 10X were found to be negatively charged at a weight ratio of 0.3, neutral at 0.5, and retain positive charge of approximately 30 mv at a weight ratio above 5. It was thought to be due to the higher charge density of HECP2k 5X and 10X than 1X. The average size and zeta-potential value of HECP2k were proper for access to the negatively charged cell membranes and cellular uptake of the polyplexes [46, 47].

(A)

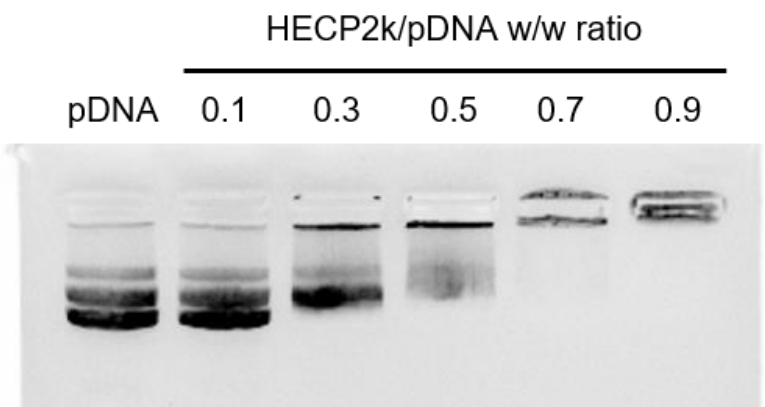

(B)

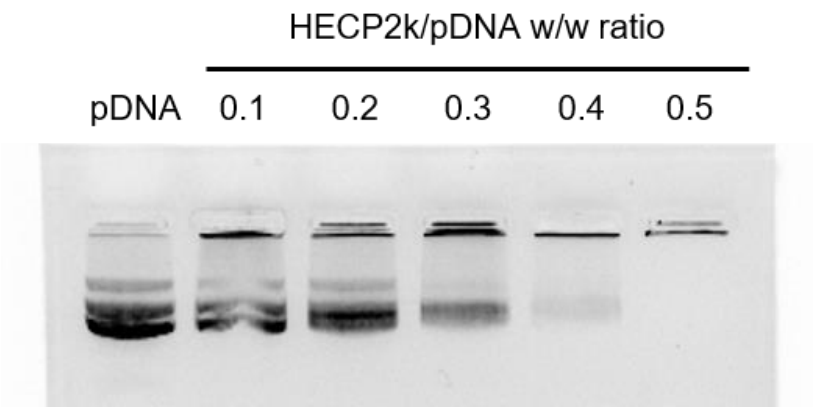

(C)

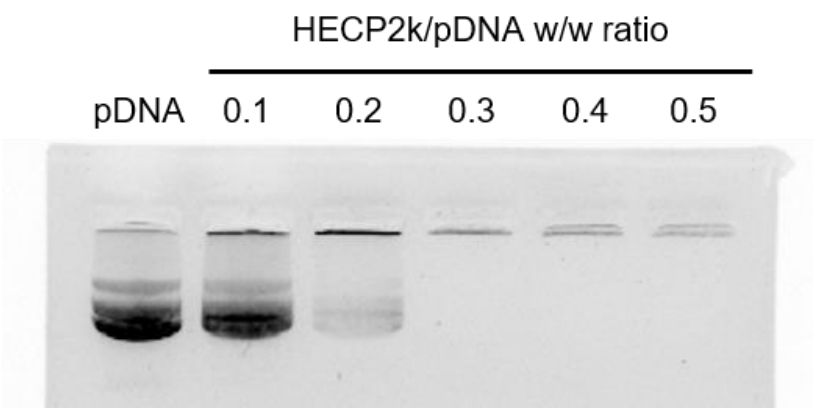

Figure 9. Agarose gel electrophoresis of (A) HECP2k 1X, (B) HECP2k 5X, (C) HECP2k 10X.

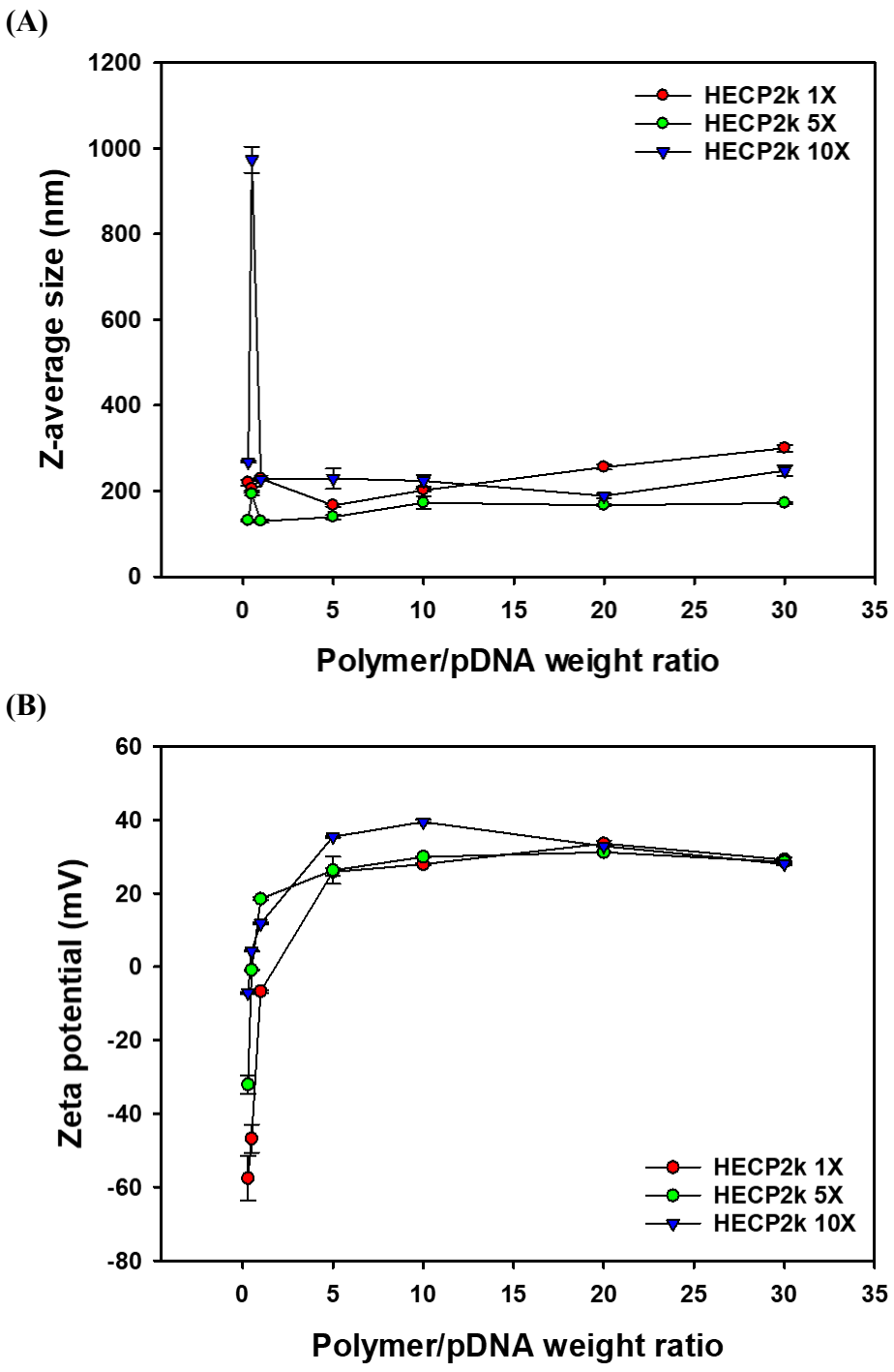

Figure 10. (A) Z-average size and (B) zeta-potential values of HECP2k/pDNA polyplexes.

4.3. *In vitro* assay of HECP2k and HECP2k/pDNA polyplex

4.3.1. Cell metabolic activity with MTT assay

The cytotoxicity of HECP2k was estimated by investigating cell metabolic activity with MTT assay (Figure 11). HeLa cells and HepG2 cells were used for the cytotoxicity test. Relative cell viability (RCV, %) was measured by assuming the activity of the untreated group as 100%.

In the case of HeLa cells (Figure 11A), PEI25k showed significant cytotoxicity even at low concentrations, although HECP2k 5X and 10X showed negligible cytotoxicity with high RCV (> 90%) at all concentrations. Interestingly, HECP2k 1X showed slight cytotoxicity compared to 5X and 10X. Cationic polymer can exhibit cytotoxicity when it has a large molecular weight or high charge density [33]. Certain cytotoxicity of HECP2k 1X was thought to be due to the high molecular weight of the polymer. According to molecular weight measurement results (4.1.3., Table 2.), the molecular weight of HECP2k 1X was highest among the HECP2k 1X, 5X, and 10X. The high molecular weight of HECP2k 1X may lead to certain cytotoxicity of HECP2k 1X.

In the case of HepG2 cells (Figure 11B), all the HECP2k showed low cytotoxicity (> 80%). Also, the RCV of PEI25k decreased gradually, due to HepG2 cells having a certain degree of low susceptibility compared to HeLa cell.

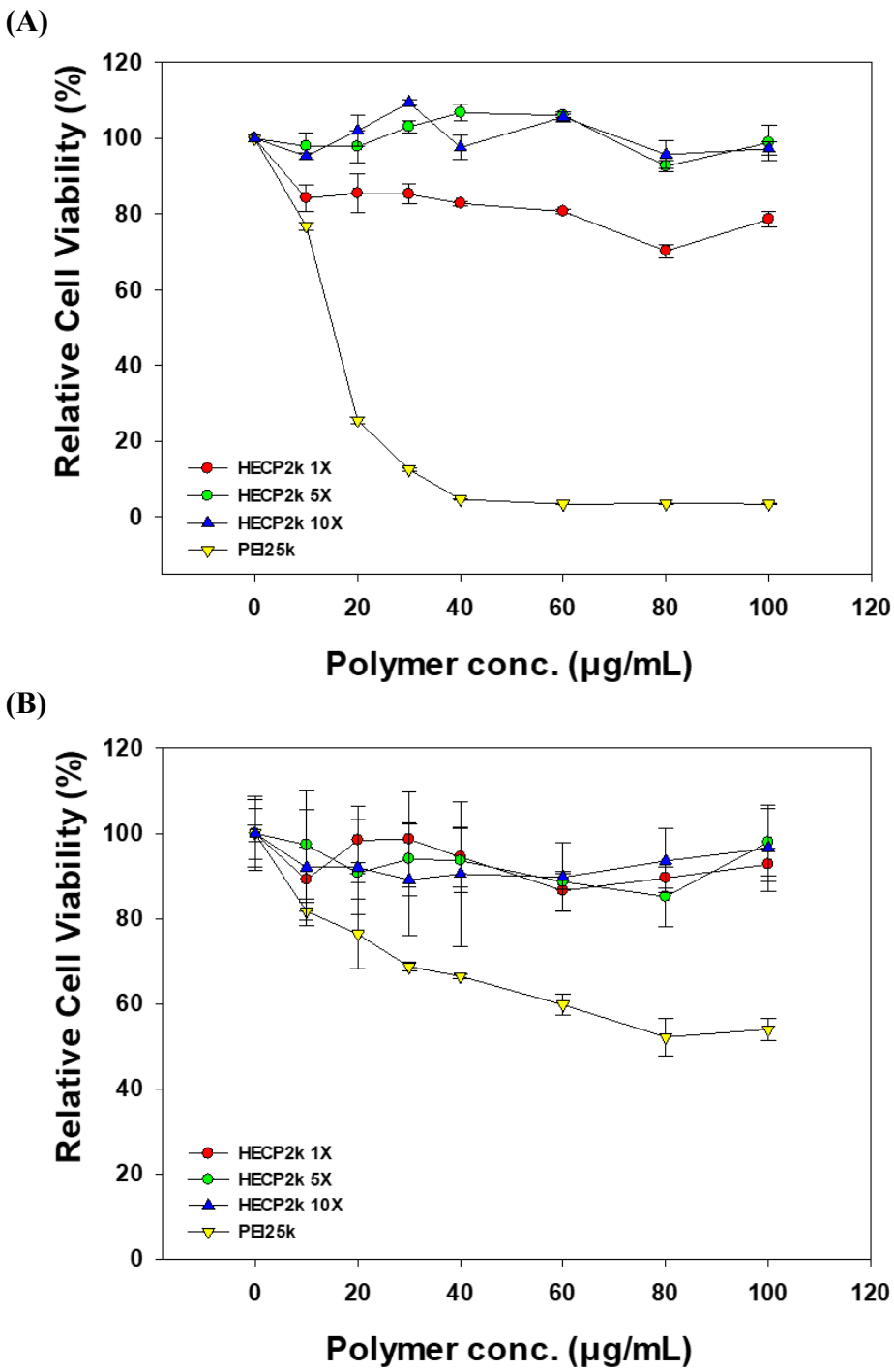

Figure 11. MTT assay results in (A) HeLa and (B) HepG2 cells.

4.3.2. Gene transfection efficiency with luciferase transgene expression assay

In order to be used for a gene delivery system, polyplex should perform transgene expression well. Transfection efficiency was examined by luciferase transgene expression assay. pCN-Luci (pDNA) was used as a reporter gene expressing luciferase protein. Luminescence from reaction with expressed luciferase and luciferin was measured, corrected by protein amounts, and presented into RLU/mg protein. The untreated group (cell) and PEI25k were used as control.

Firstly, to evaluate the general transfection efficiency of HECP2k 1X, 5X, and 10X, the assay was performed in serum-free conditions with HeLa cells. The transfection efficiency increased as the ratio of PEI and the weight ratio increased (Figure 12). Although HECP2k 1X and 5X showed lower transfection efficiency than PEI25k, HECP2k 10X showed similar transfection efficiency to PEI25k and low cytotoxicity. Therefore, later experiments were conducted by optimizing with HECP2k 10X (subsequently named HECP2k).

Due to the gradual increase of transfection efficiency with the increase of weight ratio, additional assays were performed with the extended weight ratios of 30, 50, and 70 (Figure 13). The experiments were performed in serum-free (Figure 13A) or serum conditions (Figure 13B) in HeLa cells. The transfection efficiency of HECP2k was 35–127 times higher than that of PEI25k at their weight ratio of 50 and 70 in serum-free conditions. Their transfection efficiency in serum condition was 9–19 times higher at their weight ratio of 50 and 70. These results demonstrated that HECP2k has superior transfection efficiency.

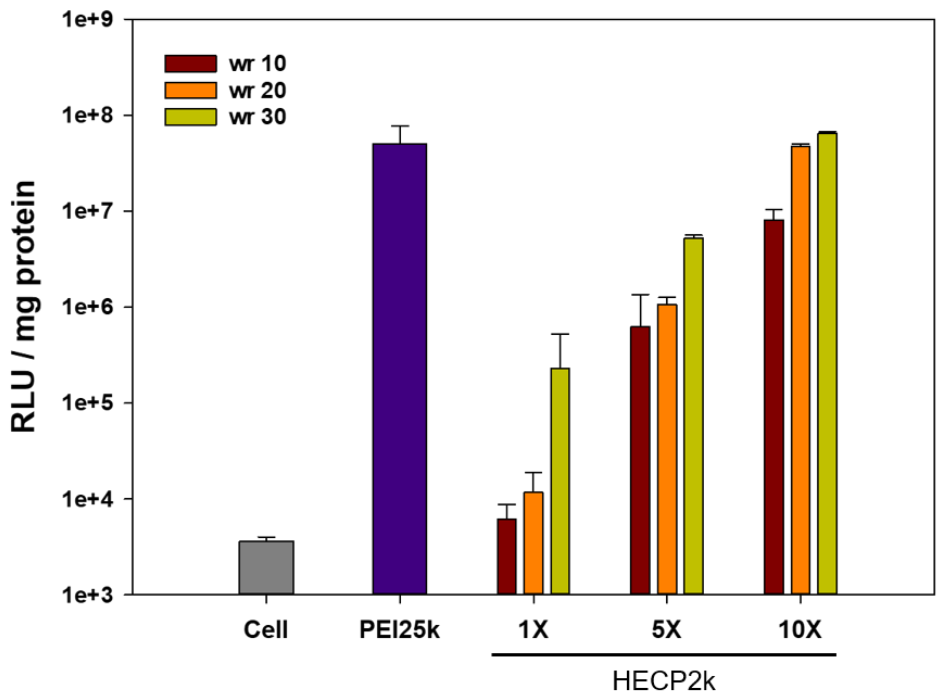

Figure 12. Luciferase assay results of PEI25k/pDNA and HECP2k/pDNA in HeLa cells at the various weight ratios of polymer/pDNA = 10, 20, 30 : 1 w/w.

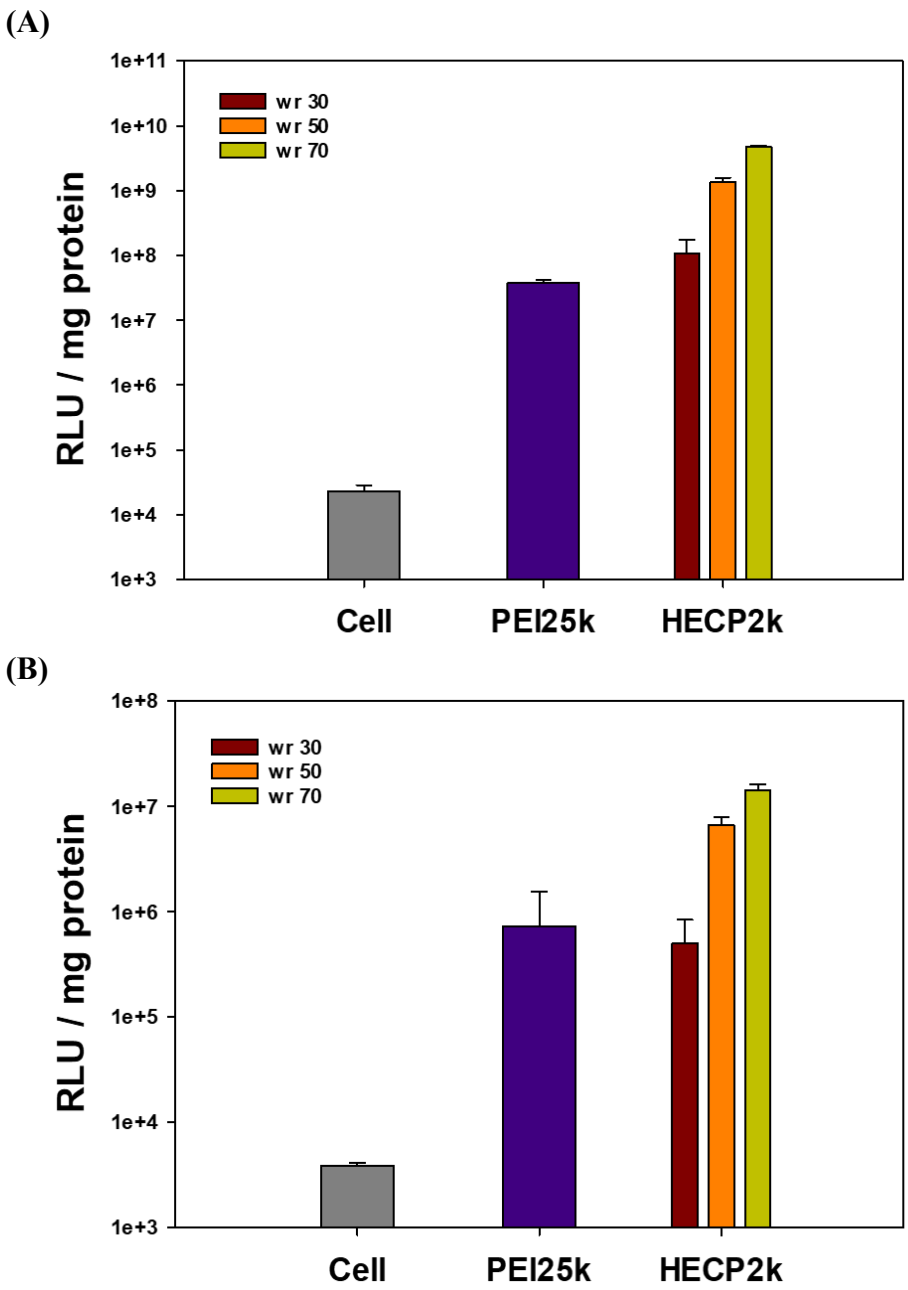

Figure 13. Luciferase assay results of PEI25k/pDNA and HECP2k/pDNA in HeLa cells at the various weight ratios of polymer/pDNA = 30, 50, 70 : 1 w/w. (A) Serum-free condition and (B) serum condition.

4.3.3. Cellular uptake measurements with Flow cytometry

Cellular uptake efficiency was estimated by using YOYO-1 iodide labeled pDNA (Figure 14). The Untreated group (cell) and PEI25k were used as control. To evaluate the cellular uptake efficiency of HECP2k, two parameters were examined; relative cellular uptake (%) and normalized mean fluorescence. Firstly, relative cellular uptake (%) was examined by measuring the population of fluorescent cells. pDNA uptake was analyzed by gating in the histogram of YOYO-1 fluorescence. Fluorescent cells were gated by the top 0.1% fluorescent signal of untreated cells. While, the mean fluorescence of each sample was normalized by the fluorescence of untreated cells.

HECP2k and PEI25k were similar in relative cellular uptake (%) and the population of fluorescent cells (about 90%). The normalized mean fluorescence of HECP2k was 1.7–1.9 times higher than PEI25k. It may result from the water retainability of HEC. Water retention and hydration of HEC can cause osmotic pressure near the cellular membrane [48]. It has been reported that osmotic stress to cells could induce caveolae-mediated endocytosis via stimulating caveolin-1 (Cav-1) [49, 50]. Also, the higher transfection efficiency of HECP2k was thought to be due to the amount of uptake of genes.

Considering cytotoxicity, transfection efficiency, cellular uptake efficiency, and amount of polymer needed, the weight ratio of 50 was regarded as an optimized weight ratio for later experiments.

4.3.4. Intracellular trafficking visualization with CLSM

To observe the intracellular trafficking of polyplex, CLSM was conducted

(Figure 15). pDNA was labeled with YOYO-1 iodide (green), acidic organelles were labeled with Lysotracker red DND-99 (red), and nuclei were labeled with DAPI (blue). Intracellular uptake was observed to occur in most cells in both PEI25k and HECP2k polyplexes. This result corresponds to the previous result that about 90% of the cells were intracellularly permeated. In the case of PEI25k, the distribution of green fluorescence was mainly located in the cytosol at 0 h, 2 h, and 4 h after treatments (Figure 15A, C, E). Whereas HECP2k showed cytosol-located green fluorescence right after treatment (Figure 15B), but green fluorescence located near nuclei at 2 h and 4 h after treatments (Figure 15D, F). Also, Green fluorescence in nuclei was observed at 4 h after treatment for HECP2k (Figure 15G). In addition, there were few cells containing the co-localized signal. This may be due to their fast endosome escape. These results correlated with previous cellular uptake measurements (4.3.3, Figure 14) and demonstrated that HECP2k showed superior intracellular trafficking behaviors to PEI25k.

(A)

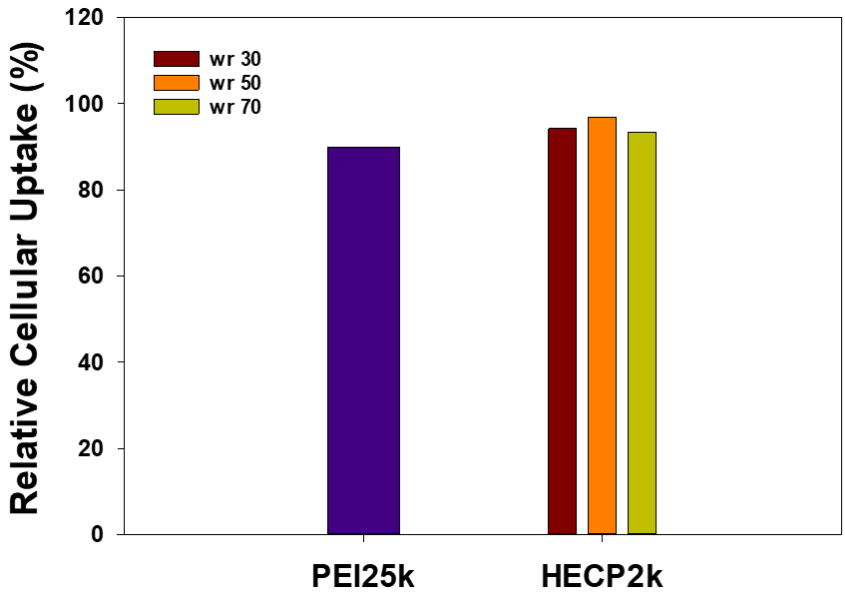

(B)

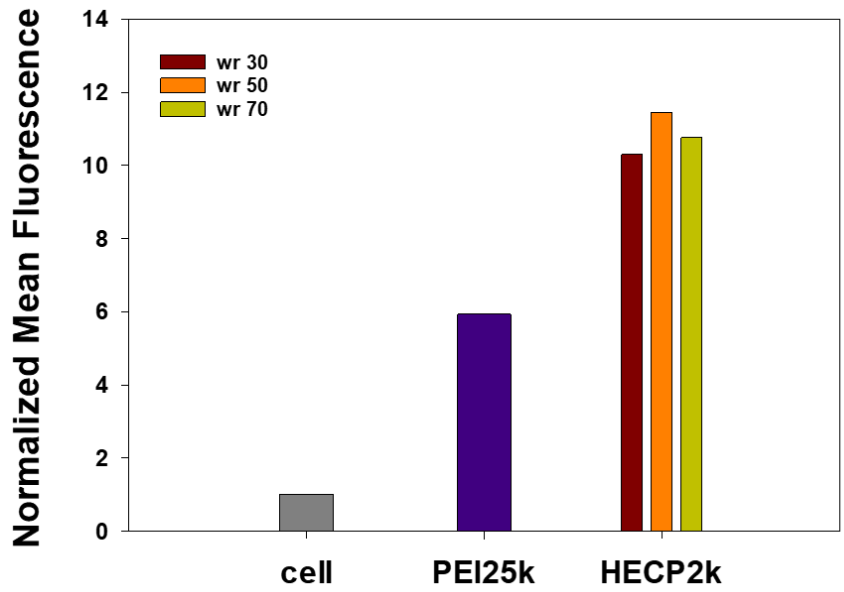

Figure 14. Flow cytometry results of PEI25k/pDNA and HECP2k/pDNA in HeLa cells at various weight ratios of polymer/pDNA = 30, 50, 70 : 1 w/w. (A) Relative cellular uptake and (B) Normalized mean fluorescence unit.

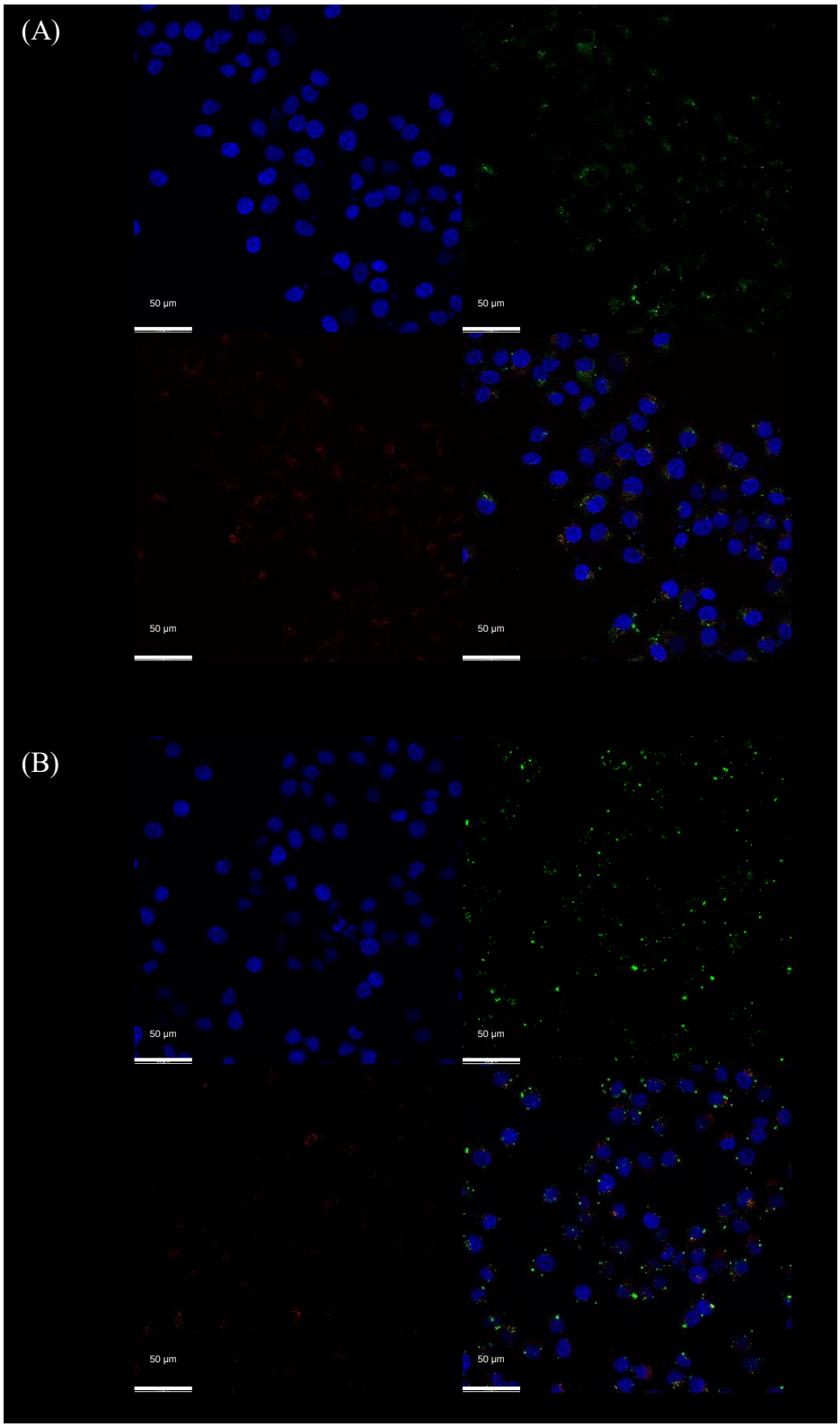
(A)
50 μm
50 μm
50 μm
50 μm
(B)
50 μm
50 μm
50 μm
50 μm

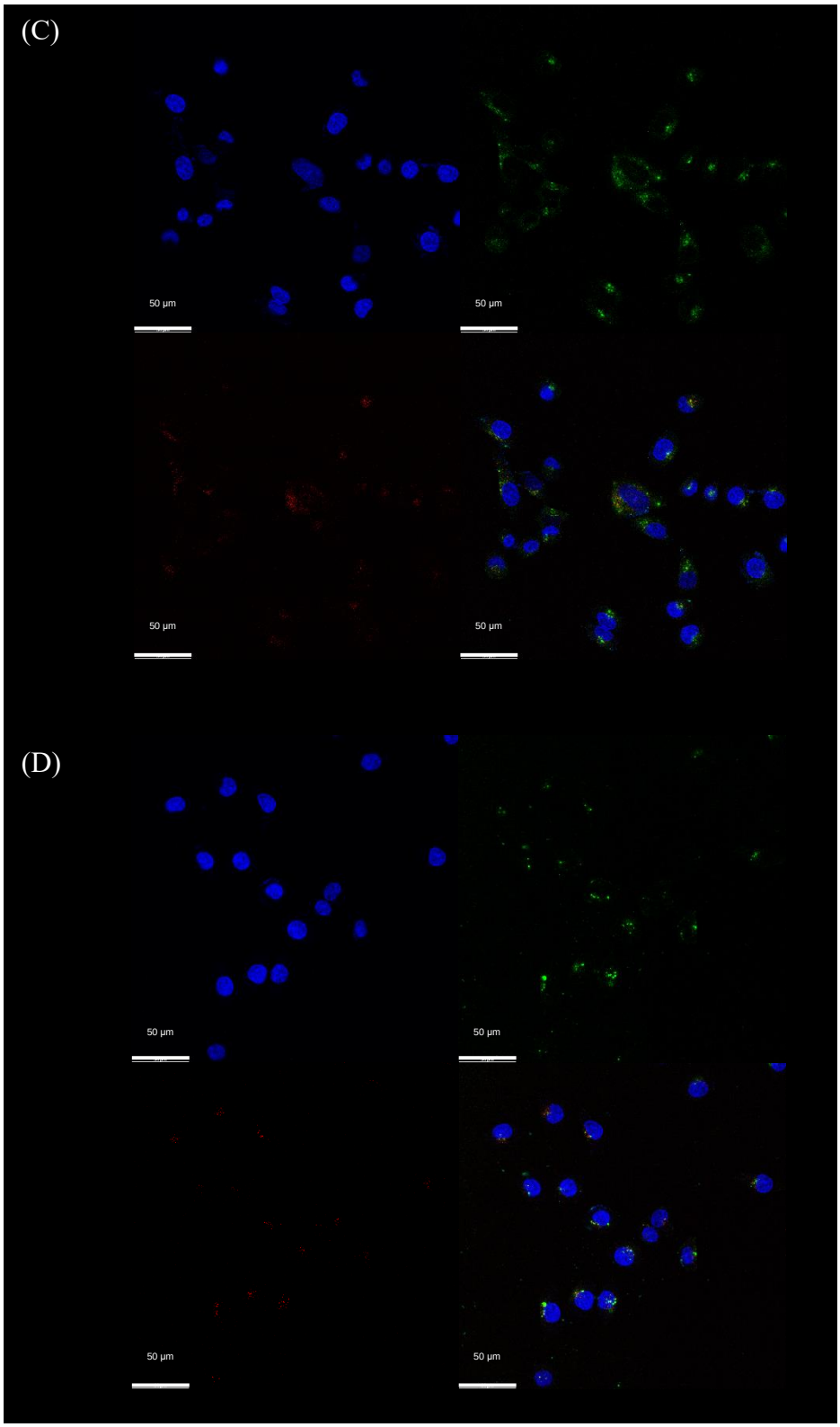
(C)
50 μm
50 μm
50 μm
50 μm
(D)
50 μm
50 μm
50 μm
50 μm

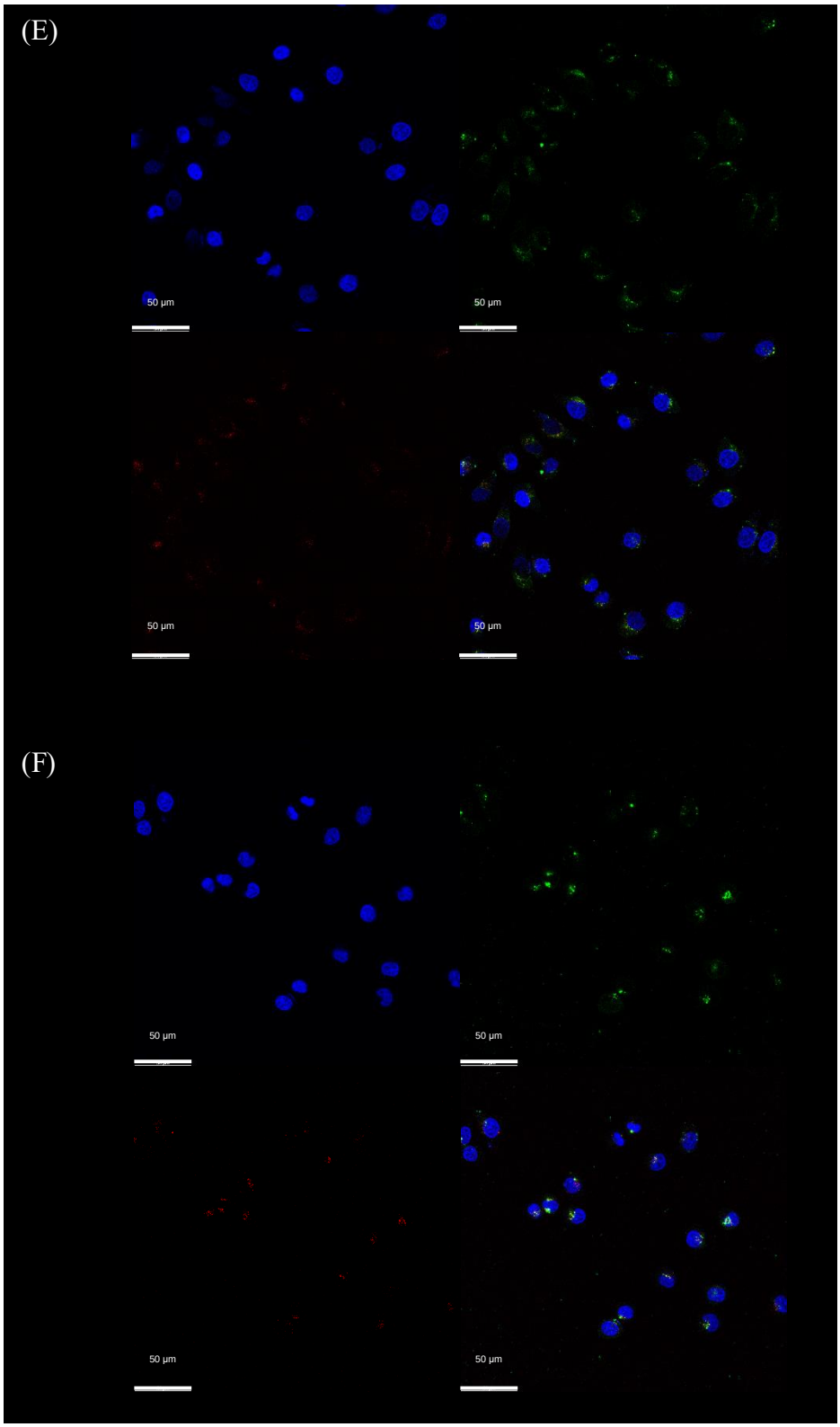
(E)
50 μm
50 μm
50 μm
50 μm
(F)
50 μm
50 μm
50 μm
50 μm

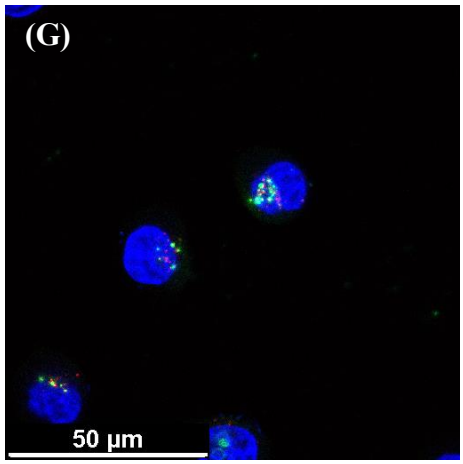

Figure 15. CLSM images of PEI25k/pDNA (A, C, E) and HECP2k/pDNA polyplexes (B, D, F, G) in HeLa cells. pDNA was labeled by YOYO-1 (green). DAPI (blue) stained nuclei and Lysotracker red DND-99 (red) stained acidic organelles. After 4 h of treatments, cells were visualized after (A, B) 0 h, (C, D) 2 h, (E, F) 4 h of further incubation. (G) is magnified merge image of (F).

4.3.5. Serum stability test

To estimate serum stability, the transfection efficiencies of HECP2k polyplexes in 10%, 30%, and 50% FBS conditions were measured by luciferase transgene expression assay (Figure 16). PEI25k polyplexes were used as control. As shown in Figure 16, the transfection efficiency of PEI25k decreased drastically as the concentration of FBS increased. In 50% FBS condition, PEI25k polyplexes showed low transfection efficiency similar to the untreated group (cell). Whereas, in the case of the HECP2k polyplex, the tendency to decrease the transfection efficiency was alleviated compared to PEI25k. HECP2k retained their transfection efficiency up to 85.4 times higher than PEI25k polyplex under 50% FBS concentration. This result demonstrated that the HECP2k polyplex had great serum stability compared to PEI25k polyplex. It was thought to be due to the ethylene oxide groups on the structure of HEC hampered serum protein to cohering with the polyplexes.

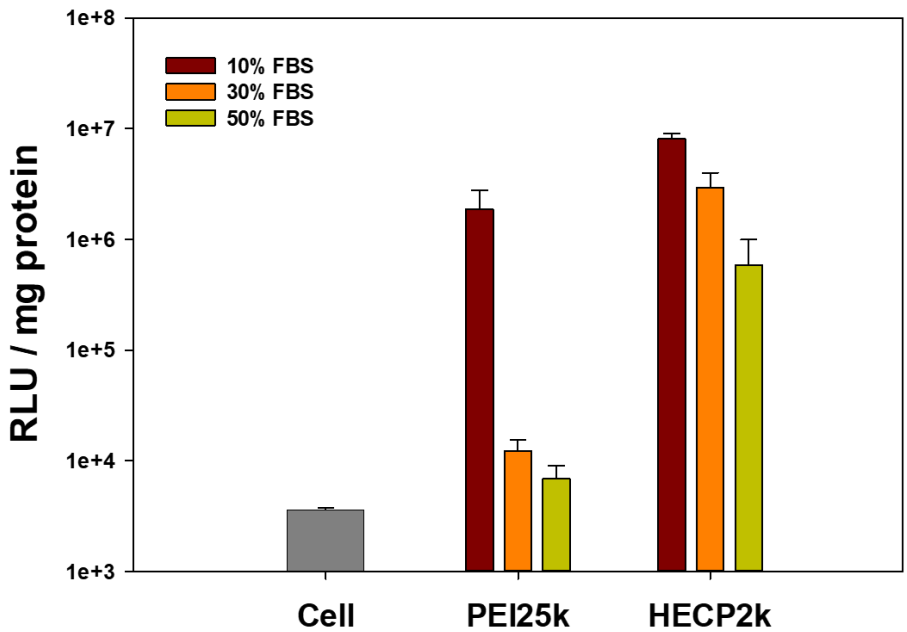

Figure 16. Serum stability test results of PEI25k/pDNA and HECP2k/pDNA polyplexes by luciferase assay.

4.4. Antitumor effect of HECP2k@Dox/siRNA

4.4.1. Drug loading contents and drug loading efficiency measurements

The anticancer agent, Doxorubicin (Dox) was encapsulated in HECP2k by dialysis method [51]. Despite doxorubicin is hydrophobic, the encapsulation could be caused by interaction with the polymer including hydrogen bonding or physical embedding [51, 52, 53]. The absorbance at 570 nm was measured by a microplate reader. The calibration curve was drawn based on doxorubicin in a solvent where water and DMSO were mixed at a ratio of 10:90 (Figure 17). The same solvent was used for the analysis. When the mixing ratio (Dox/HECP2k, w/w) was 3/10, the drug loading efficiency (DLE) of Dox-loaded HECP2k (HECP2k@Dox) was 41.49% and drug loading content (DLC) was 13.83% (Table 3).

4.4.2. Average size and zeta-potential measurements with DLS

The Average size and zeta-potential value of HECP2k/siRNA polyplexes and HECP2k@Dox/siRNA complexes at an optimized weight ratio of 50 were measured (Table 4). The average size and zeta-potential value of HECP2k/siRNA were 153.7 ± 3.0 nm and 14.7 ± 2.4 mV, respectively. After the doxorubicin encapsulation, the average size and zeta-potential value of HECP2k@Dox/siRNA were 241.3 ± 0.1 nm and 17.00 ± 0.8 mV, respectively, which were proper size and surface charge for cellular uptake. The size of HECP2k@Dox/siRNA is a bit larger for clathrin-mediated, caveolin-mediated, or clathrin/caveolin-independent

endocytosis, but there are other possible pathways such as macro-pinocytosis [54, 55].

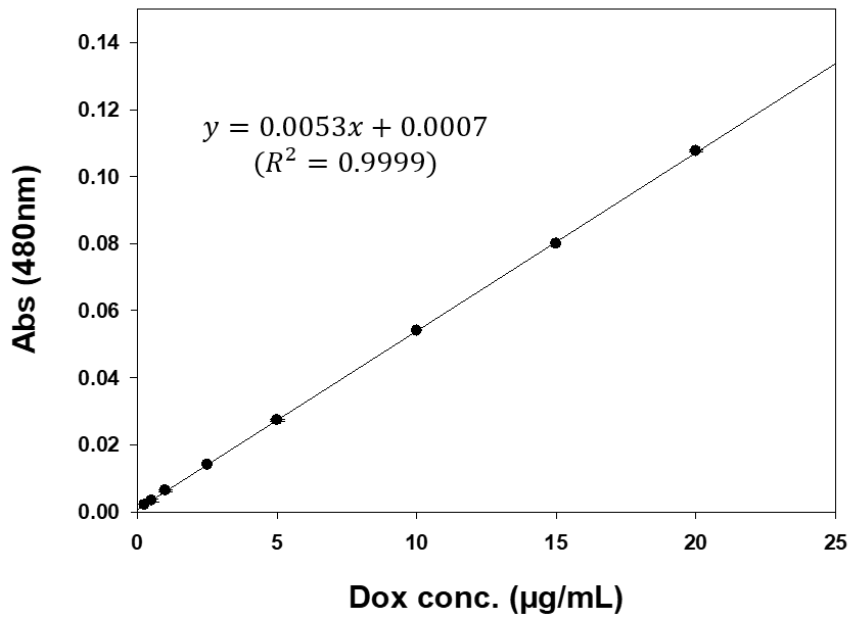

Figure 17. Calibration curve for Dox loading content and Dox loading efficiency measurements.

Table 3. Drug loading content and drug loading efficiency of HECP2k@Dox.

	Drug Loading Content (%)	Drug Loading Efficiency (%)
HECP2k@DOX	13.83	41.49

Table 4. Z-average size and zeta-potential values of HECP2k/siRNA polyplexes and HECP2k@Dox/siRNA nanocomplexes.

Sample	Size (nm)	Zeta-potential (mV)
HECP2k/siRNA	153.7 ± 3.0	14.67 ± 2.39
HECP2k@Dox/siRNA	241.3 ± 0.1	16.97 ± 0.76

4.4.3. Antitumor effect analysis with MTT assay

Antitumor effect of HECP2k@Dox/siRNA complexes was investigated by MTT assay in HeLa and HepG2 cells in order to identify the combinatorial effect for co-delivery of Dox and siRNA for non-MDR (HeLa) or MDR (HepG2) cells [56, 57], respectively (Figure 18). Each concentration of Dox and siRNA is shown in Table 5. In HeLa cells (Figure 18A), free Dox showed a strong cancer cell-killing effect. Free siRNA could not induce any cytotoxic effect on HeLa cells because of the very low delivery efficiency by the absence of the carrier. PEI25k/siRNA-treated group also showed a low cancer cell-killing effect. In the case of HECP2k/siRNA, they showed a higher cancer cell-killing effect compared to PEI25k/siRNA. It was thought to be due to the higher transfection efficiency of HECP2k than PEI25k. HECP2k@Dox exhibited 48.48% cell viability at a high concentration (15 μg/mL). HECP2k@Dox/siRNA could reduce the cell viability to 42.08% at a high concentration (15 μg/mL). In HepG2 cells (Figure 18B), free Dox showed above 60% cell viability even treated at a high concentration (15 μg/mL) because of the MDR property of HepG2 cells. Except for free siRNA, the cell viability decreased as the concentration increased. Among them, HECP2k@Dox was the only group that exhibited cell viability less than 50%.

A median effect analysis was conducted to construct the median effect plot. The method of plotting was referred to the works of T. C. Chou [58] and T. Zhang [59]. Briefly, dose-effect curves were constructed based on previous MTT assay results (Figure 20A, B). The dose and effect relations could be linearized by plotting log (dose) vs. log [fraction affected (f_a) / fraction unaffected (f_u)] (Figure 20C, D, E, F). Based on the median-effect equation, the theoretical minimum of constructing

a dose-effect curve requires only two data points. The median-effect equation is shown below.

$$\frac{fa}{fu} = \left(\frac{D}{Dm}\right)^m$$

$fa =$ fraction of system affected
$fu = (1 - fa) =$ fraction unafftected
$D =$ dose required to produce fa
$Dm =$ dose required to produce median effect. i.e. IC50
$m =$ dynamic order (shape)

Based on the median effect plots (Figure 20C, D, E, F), the combination index (CI) was calculated (Figure 21). Values of CI > 1, = 1, < 1 indicate antagonism, additive effect, and synergism, respectively. As for HeLa cells (Figure 21A), synergism was shown up at 0.2 or less affected fractions, but it showed enormous antagonism above that. This result was thought to be due to the non-MDR characteristics of HeLa cells, which contributed to the strong cytotoxicity of Dox itself. Since the affected fraction below 0.2 is not valuable as cancer treatment, HECP2k may be considered difficult to expect a synergistic effect for HeLa cells. Whereas for HepG2 cells (Figure 21B), synergism was shown up at 0.2 or more affected fractions. These results demonstrated that co-delivery of Dox with Bcl-2 siRNA could exhibit synergism which may be due to the diminution of MDR characteristics by down-regulation of Bcl-2 proteins. Therefore, HECP2k for co-delivery of Dox with Bcl-2 siRNA could be considered a therapeutic delivery system with great potential.

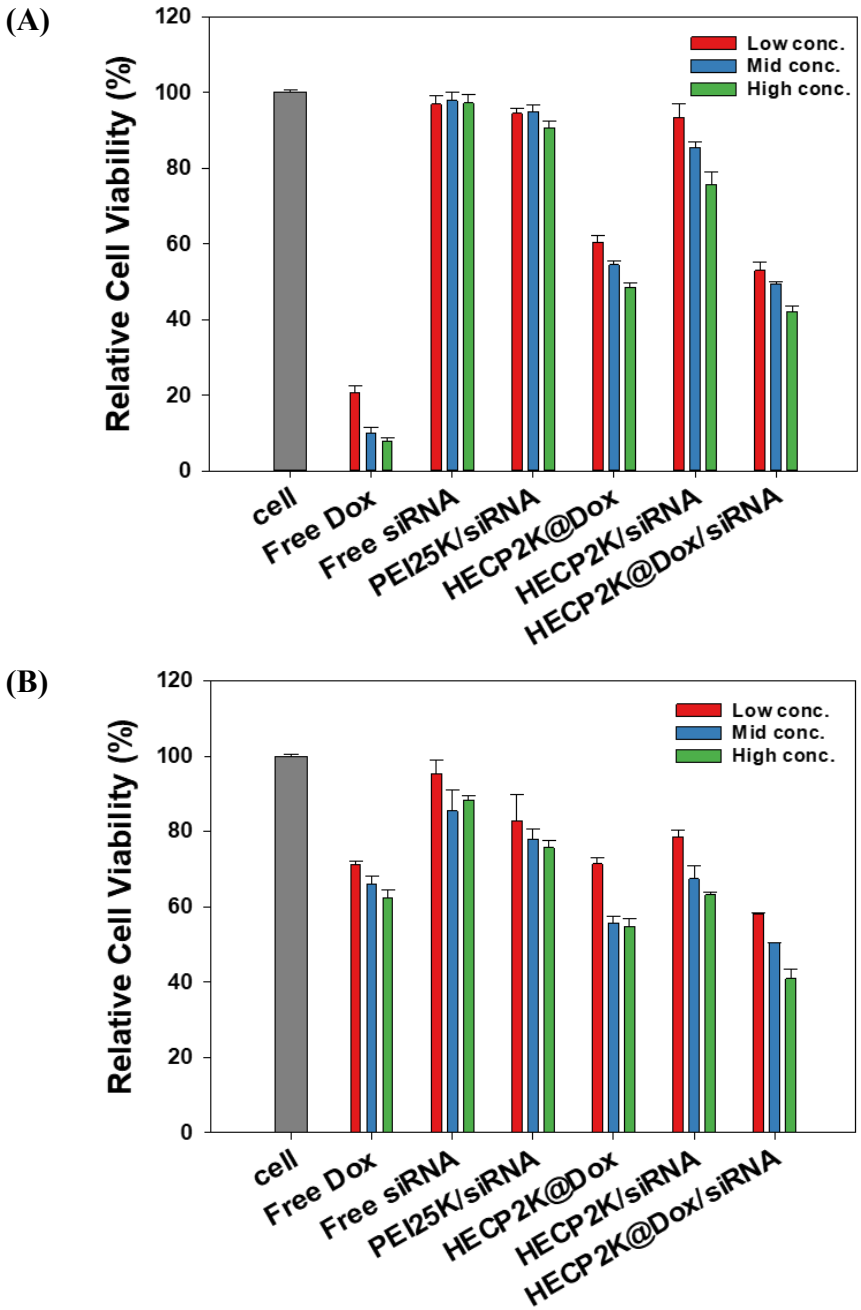

Figure 18. MTT assay results showing antitumor effects of free dox, free siRNA, PEI25k/siRNA, HECP2k@Dox, HECP2k/siRNA, HECP2k@Dox/siRNA nanocomplexes in (A) HeLa and (B) HepG2 cells. (Three different conditions of the concentration were described in Table 5.)

Table 5. Chart of Dox and Bcl-2 siRNA concentration for each condition.

HECP2k@DOX	Dox conc. (ug/mL)	siRNA conc. (ug/mL)
Low conc.	4	0.5
Mid conc.	7	1
High conc.	15	2

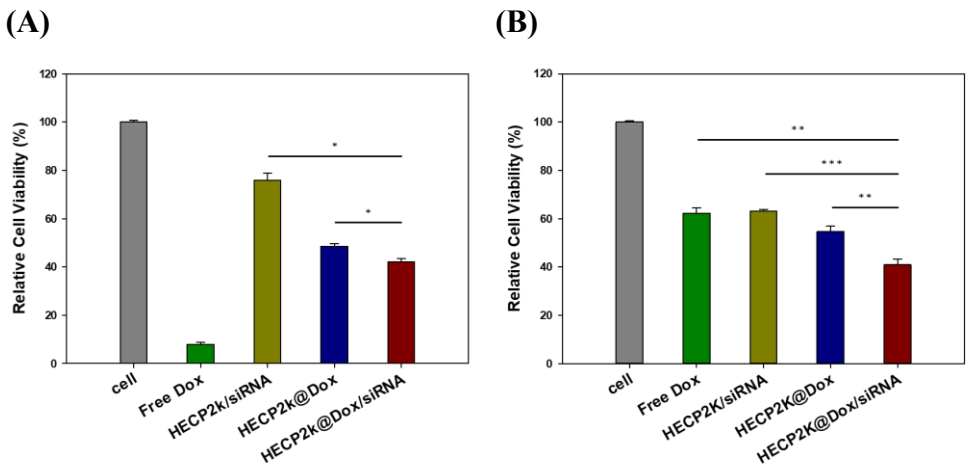

Figure 19. Relative cell viability for free Dox, HECP2k/siRNA, HECP2k@Dox/siRNA nanocomplexes at a high concentration of Dox and siRNA in (A) HeLa and (B) HepG2 cells. Statistical analysis was proceeded through one-way ANOVA and Bonferroni post-hoc test. Statistical significance was presented as follows. ($P<0.05$ *, $P<0.01$ **, $P<0.001$ ***)

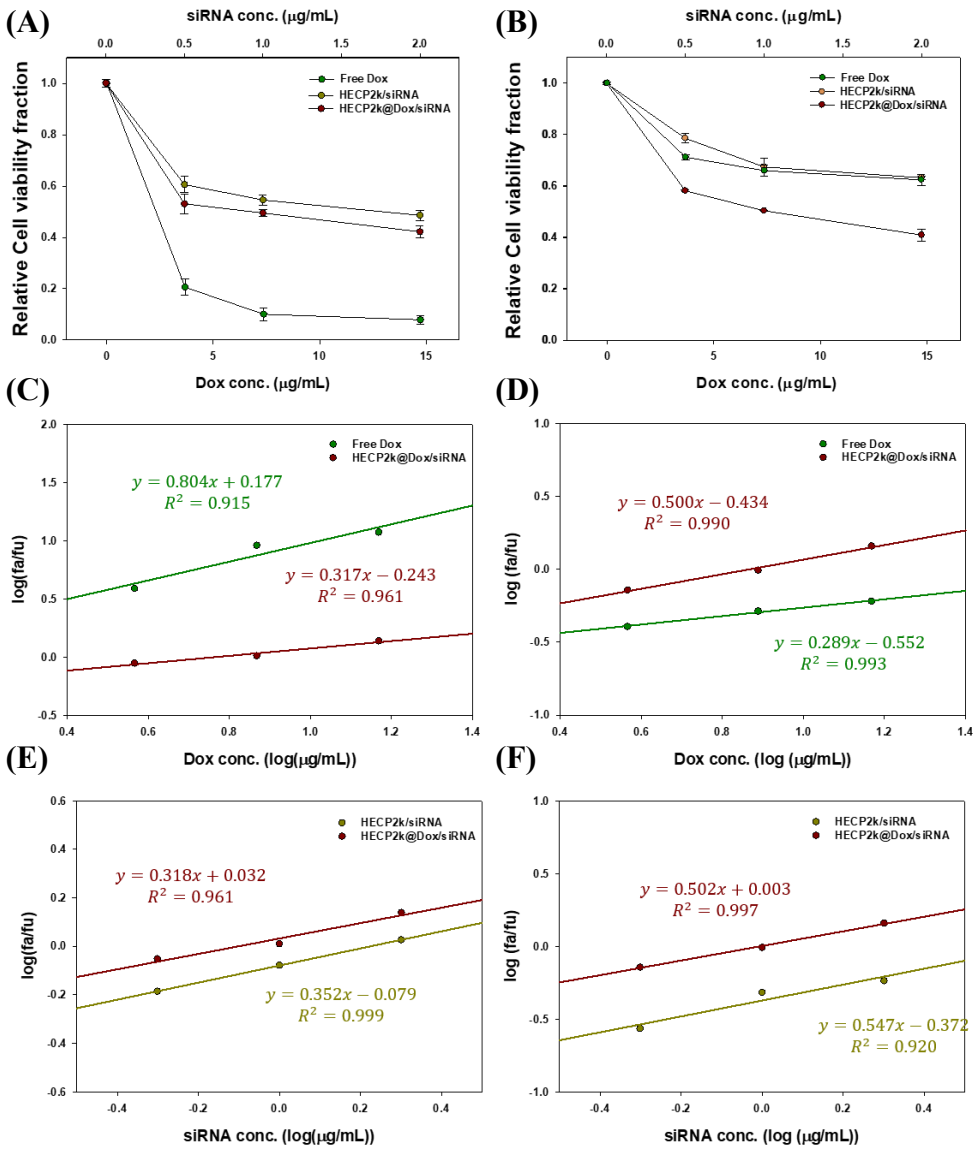

Figure 20. Dose-effect curves of Dox and siRNA in (A) HeLa and (B) HepG2 cells. Median effect plots for Dox in (C) HeLa and (D) HepG2 cells. Median effect plots for Bcl-2 siRNA in (E) HeLa and (F) HepG2 cells.

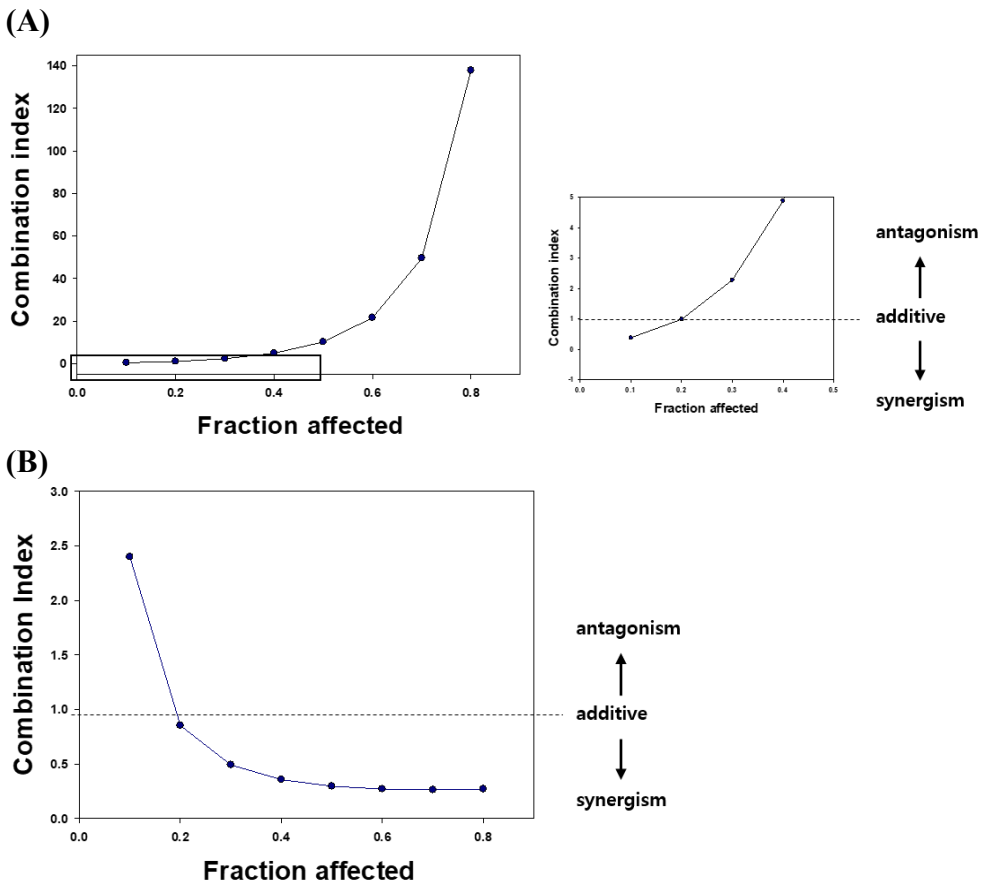

Figure 21. Combination index (CI) based on the median effect plots for (A) HeLa and (B) HepG2 cells.

4.4.4. Apoptosis induction test with Annexin V staining

In order to verify that HECP2k@Dox/siRNA complexes induce cell death through apoptosis, Annexin V staining was conducted (Figure 22). The human vascular anticoagulant annexin V is a Ca^{2+}-dependent phospholipid-binding protein that has a high affinity for the anionic phospholipid phosphatidylserine (PS). In normal healthy cells, PS is located on the cytoplasmic surface of the plasma membrane. Whereas during apoptosis, structural collapse of plasma membrane occurs, leading PS to translocate from the inner to outer side of the plasma membrane. Therefore, PS on the cell's outer surface has been used as a pro-apoptosis marker [60].

To stain the pro-apoptotic cells, Alexa fluor® 488 was used (FL1). Dead cells were stained by propidium iodide (PI, FL2). Since the fluorescent wavelength range of Alexa Fluor® 488 and PI overlapped, color compensation was conducted as FL2-7.3% FL1. As shown in Figure 22, the untreated group (Figure 22A) showed 75.0% of the cells lived, 9.2% were undergoing apoptosis, and 15.8% died spontaneously. Whereas the HECP2k@Dox/siRNA-treated group (Figure 22B) showed that only 28.9% of the cells lived, and 60.7 % died. Notably, 10.4% of the cells were found to be undergoing apoptosis, while other cells have completed apoptosis. This result demonstrated that HECP2k@Dox/siRNA induced apoptosis and came into cell death

(A)

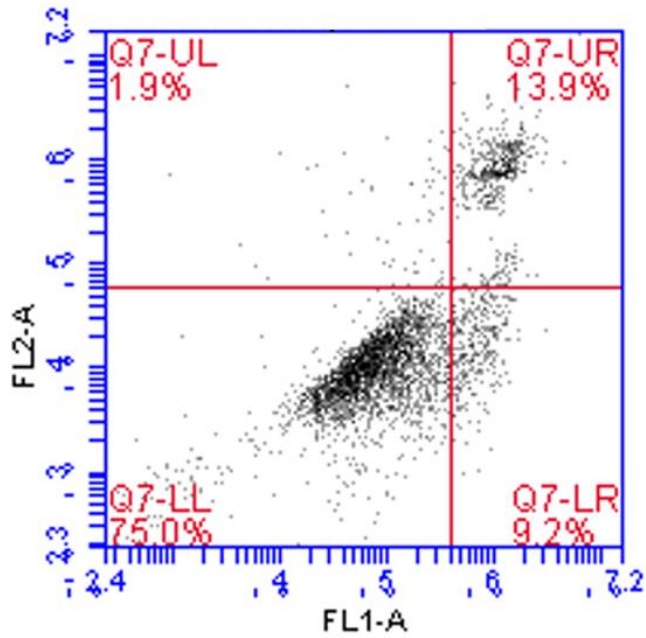

(B)

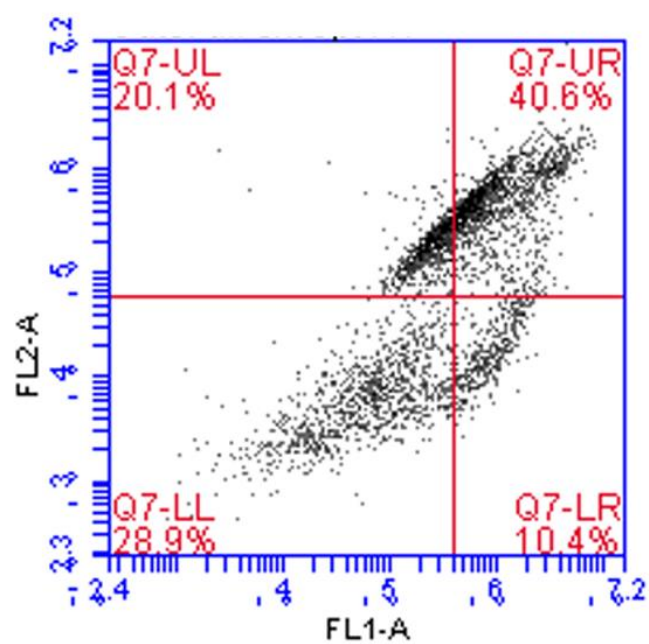

Figure 22. Flow cytometry results by annexin V staining of (A) untreated cell and (B) HECP2k@Dox/siRNA. (FL1: Alexa® Fluor 488, FL2: PI)

5. Conclusion

This study suggested the potential of HECP2k, the PEI-conjugated hydroxyethyl cellulose, for Bcl-2 siRNA/doxorubicin co-delivery systems. In order to synthesize HECP2k, hydroxyethyl cellulose (HEC) was oxidized using sodium periodate and conjugated with low molecular weight polyethylenimine (PEI, Mw 2000) through reductive amination. The chemical structure of HECP2k was analyzed by ^{1}H NMR, primary amine quantification, ^{13}C NMR, and FT-IR. The conjugation ratios of PEI were increased as the feed ratio of PEI increased. The discordance between amounts of primary amine by fluorescamine and that of ^{1}H NMR can be considered due to the unreacted primary amine with fluorescamine by the steric hinderance. Using GPC, the molecular weights of HECP2k were measured, and successful purification of the polymer was confirmed. Molecular weights of HECP2k decreased as the conjugation ratio of PEI increased. Namely, HECP2k 1X showed the highest molecular weight among the three samples. This could be explained by that an excess amount of PEI disrupted stoichiometric balance, which caused a decrease in Mw. Also, HECP2k/pDNA polyplex showed the proper size and zeta-potential value for access to the negatively charged cell membrane and cellular uptake of the polyplexes.

Prior to applying HECP2k to a drug/gene co-delivery system, the properties and potential of HECP2k were examined as a gene delivery system. HECP2k showed low cytotoxicity in both HeLa and HepG2 cells due to intrinsic biocompatibility of HEC and low cytotoxicity of PEI2k. Also, it was examined that HECP2k had excellent transfection efficiency due to the serum stability and cellular uptake properties. HECP2k showed superior cellular uptake efficiency. This could be due to

water retention and hydration of HEC, which can induce endocytosis via stimulating Cav-1. The transfection efficiency of the HECP2k/pDNA polyplex was relatively stable compared to PEI25k/pDNA polyplex despite of the high content of serum protein in the treated medium. Therefore, it was identified that HECP2k had great potential to be used for gene delivery carriers.

An anticancer agent, doxorubicin, was encapsulated in the HECP2k to form HECP2k@Dox. The proper particle size and surface charge of HECP2k/siRNA and HECP2k@Dox/siRNA were confirmed. HECP2k@Dox/Bcl-siRNA nanocomplex was applied and analyzed for its antitumor effect. Through the co-delivery of Bcl-2 siRNA and doxorubicin, the nanocomplex synergistically improved the antitumor effect in HepG2 cells. In order to assess apoptosis induction of HECP2k@Dox/siRNA, Annexing V staining experiment was conducted. As a result, HECP2k@Dox/siRNA could induce apoptosis, which caused cell death.

Consequently, a new antitumor complex was developed, and its properties and potential, proven from high gene transfection efficiency and improved antitumor effect, were suggested. It is expected that various research could be conducted based on this study.

References

[1] L. Jin, Current progress in gene delivery technology based on chemical methods and nano-carriers, Theranostics, 2014, 4 (3), 240–255

[2] P. Zhang, and E. Wagner, History of Polymeric Gene Delivery Systems, Topics in Current Chemistry, 2017, 375, 26

[3] S. Y. Wong, J. M. Pelet, and D. Putnam, Polymer systems for gene delivery-Past, present, and future, Progress in Polymer Science, 2007, 32 (8–9), 799–837

[4] Q. Yin, J. Shen, L. Chen et al., Overcoming multidrug resistance by co-delivery of Mdr-1 and surviving-targeting RNA with reduction-responsible cationic poly(β-amino esters), Biomaterials, 2012, 33 (27), 6495–6506

[5] M. S. Singh, S. N. Tammam, M. A. S. Boushehri, and A. Lamprecht, MDR in cancer: Addressing the underlying cellular alterations with the use of nanocarriers, Pharmacological Research, 2017, 128, 2–30

[6] Q. J. He, Y. Gao, L. X. Zhang et al., A pH-responsive mesoporous silica nanoparticles-based multi-drug delivery system for overcoming multi-drug resistance, Biomaterials, 2011, 32, 7711–7720

[7] H. J. Cho, H. Y. Yoon, H. Koo et al., Self-assembled nanoparticles based on hyaluronic acid-ceramide (HA-CE) and Pluronic® for tumor-targeted delivery of docetaxel, Biomaterials, 2011, 32, 7181–7190

[8] D. Vergara, C. Bellomo, X. Zhang et al., Lapatinib/Paclitaxel polyelectrolyte nanocapsules for overcoming multidrug resistance in ovarian cancer, Nanomedicine, 2012, 8 (6), 891–899

[9] A. M. Eissa, E. Khosravi, A. L. Cimecioglu, A versatile method for functionalization and grafting of 2-hydroxyethyl cellulose (HEC) via click chemistry, Carbohydrate Polymers, 2012, 90 (2), 859–869

[10] D. Trache, M. H. Jussin, M. K. Mohamad Haafiz et al., Recent progress in cellulose nanocrystals: sources and production, Nanoscale, 2017, 9 (5)

[11] P. B. Lawrence, J. L. Price, How PEGylation influences protein conformational stability, Current Opinion in Chemical Biology, 2016, 34, 88–94

[12] M. Mahdavi, A. Fattahi, S. Nouranian, Doxorubicin stability and retention on PEGylated graphene oxide nanocarriers adjacent to human serum albumin, Applied Bio Materials, 2020, 3 (11), 7646–7653

[13] N. Ding, Y. Wang, X. Wang et al., Improving plasma stability and antitumor effect of gemcitabine via PEGylated liposome prepared by active drug loading, Journal of Drug Delivery Science and Technology, 2020, 57, 101538

[14] A. Zakeri, M. A. Kouhbanani, N. Beheshtkhoo et al., Polyethylenimine-based nanocarriers in co-delivery of drug and gene: a developing horizon, Nano Reviews & Experiments, 2018, 9 (1), 1388397

[15] U. Lungwitz, M. Breunig, T. Blunk et al., Polyethylenimine-based non-viral gene delivery systems, European Journal of Pharmaceutics and Biopharmaceutics, 2005, 60 (2), 247–266

[16] Y. Hu, B. H. Xu, J. J. Xu et al., Synthesis of mannosylated polyethylenimine and its potential application as cell-targeting non-viral vector for gene therapy, Polymers, 2014, 6 (10), 2573–2587

[17] D. Hanahan and R. A. Weinberg, The hallmarks of cancer, Cell, 2000, 100 (1), 57–70

[18] S. Cory, D. C. Huang, J. M. Adams, The Bcl-2 family: role in cell survival and

oncogenesis, Oncogene, 2003, 22 (53), 8590–8607

[19] K. W. Yip, J. C. Reed, Bcl-2 family proteins and cancer, Oncogene, 2008, 27, 6398–6408

[20] J. J. Yunis, M. G. Mayer, M. A. Arnesen et al., Bcl-2 and other genomic alterations in the prognosis of large-cell lymphoma, The New England Journal of Medicine, 1989, 320 (16), 1047–1054

[21] O. Hermine, C. Haioun, E. Lepage et al., Prognostic significance of bcl-2 protein expression in aggressive non-Hodgkin's lymphoma. Groupe d'Etude des lymphomes de l'Adulte (GELA), Blood, 1996, 87 (1), 265–272

[22] R. D. Gascoyne, S. A. Adomat, S. Krajewski, Prognostic significance of Bcl-2 protein expression and Bcl-2 gene rearrangement in diffuse aggressive non-Hodgkin's lymphoma, Blood, 1997, 90 (1), 244–251

[23] U. Akar, A. Chaves-Rayes, M. Barria et al., Silencing of Bcl-2 expression by small interfering RNA induces autophagic cell death in MCF-7 breast cancer cells, Autophage, 2008, 4 (5), 669–679

[24] I. Tekedereli, S. N. Alpay, U. Akar et al, Therapeutic silencing of Bcl-2 by systemically administered siRNA nanotherapeutics inhibits tumor growth by autophagy and apoptosis and enhances the efficacy of chemotherapy in orthotopic xenograft models of ER (-) and ER (+) breast cancer, Molecular Therapy Nucleic Acids, 2013, 2 (9), e121

[25] Khan, W. Hosseinkhani, H. Ickowicz et al., Polysaccharide gene transfection agents, Acta Biomaterialia, 2012, 8 (12), 4224–4232

[26] K. Kim, K. Ryu, T-I Kim, Cationic methylcellulose derivative with serum-compatibility and endosome buffering ability for gene delivery systems, Carbohydrate Polymers, 2014, 110, 268–277

[27] J. Zhou, Y. Qin, S. Liu et al., Homogenous synthesis of hydroxyethylcellulose in NaOH/Urea aqueous solution, Macromolecular Bioscience, 2006, 6 (1), 84–89

[28] M. K. Grun, A. Suberi, K Shin et al., PEGylation of poly(amine-co-ester) polyplexes for tunable gene delivery, Biomaterials, 2021, 272 (120780)

[29] F. Fayazpour, B. Lucas, C. Alavrez-Lorenzo et al., Physicochemical and transfection properties of cationic hydroxyethylcellulose/DNA nanoparticles, Biomacromolecules, 2006, 7 (10), 2856–2862

[30] S. Himmelein, V. Lewe, M. C. A. Stuart et al., A carbohydrate-based hydrogen containing vesicles as responsive non-covalent cross-linkers, Chemical Science, 2014, 5, 1054–1058

[31] H. N. Ho, H. H. Le, T. G. Le et al., Formulation and characterization of hydroxyethyl cellulose-based gel containing metronidazole-loaded solid lipid nanoparticles for buccal mucosal drug delivery, International Journal of Biological Macromolecules, 2022, 194, 1010–1018

[32] T. G. Park, J. H. Jeong, and S. W. Kim, Current status of polymeric gene delivery systems, Advanced Drug Delivery Reviews, 2006, 58, 497–486

[33] W. T. Godbey, K. K. Wu, G. J. Hirasaki, and A. G. Mikos, Improved packing of Poly(ethylenimine)/DNA complexes increases transfection efficiency, Gene Therapy, 1999, 6, 1380–1388

[34] M. L. Forrest, J. T. Koerber, and D. W. Pack, A degradable polyethylenmine derivative with low toxicity for highly efficient gene delivery, Bioconjugate Chemistry, 2003, 14, 934–940

[35] D. Fischer, Y. Li, B. Ahlemeyer, et al., Uptake pathways and subsequent intracellular trafficking in nonviral gene delivery, Pharmacological Reviews, 2006, 58, 32–45

[36] H. M. Aldawsari, H. K. Dhaliwal, B. M. Aljaeid et al., Optimization of the conditions for plasmid DNA delivery and transfection with self-assembled hyaluronic acid-based nanoparticles, Molecular pharmaceutics, 2019, 16 (1), 128–140

[37] W. Alshaer, H. Zureigat, A. A. Karaki et al., siRNA: Mechanism of action, challenges, and therapeutic approaches, European Journal of Pharmacology, 2021, 905, 174178

[38] D. W. Malcolm, Y. Wang, C. Overby et al., Delivery of RNAi-based therapeutics for bone regeneration, Current Osteoporosis Report, 2020, 18 (3), 312–324

[39] H. Dana, G. M. Chalbatani, H. Mahmoodzadeh et al., Molecular mechanisms and biological functions of siRNA, International Journal of Biomedical Science, 2017, 13 (2), 48–57

[40] A. R. D. Delbridge, A. Strasser, The BCL-2 protein family, BH-3 mimetics and cancer therapy, Cell Death & Differentiation, 2015, 22, 1071–1080

[41] K. M. Debatin, D. Poncet, G. Kroemer, Chemotherapy: targeting the mitochondrial cell death pathway, Oncogene, 2002, 21, 8786–8803

[42] J. C. Reed, Bcl-2 family proteins and hematologic malignancies: history and future prospects, Blood, 2008, 111, 3322–3330

[43] Z. Ye, W. R. Wu, Y. F. Qin et al., An integrated therapeutic delivery system for enhanced treatment of hepatocellular carcinoma, Advanced Functional Materials, 2018, 28 (18), 1706600

[44] A. M. Chen, M. Zhang, D. Wei et al., Co-delivery of doxorubicin and Bcl-2 siRNA by mesoporous silica nanoparticles enhances the efficacy of chemotherapy in multidrug-resistant cancer cells, Small, 2009, 5 (23)

[45] O. Dragostin, L. Profire, Molecular weight of polymer used in biomedical

applications, Characterization of Polymeric Biomaterials, 2017, 5, 101–121

[46] Wagner, Ogris, and Zauner, Polylysine-based transfection systems utilizing receptor-mediated delivery, Advanced Drug Delivery Reviews, 1998, 30, 97–113

[47] I. Kopatz, J. S. Remy, and J. P. Behr. A model for non-viral gene delivery: through syndecan adhesion molecules and powered by actin, Journal of Genetic Medicine, 2004, 6, 769–776

[48] K. Arai, T. Shikata, Hydration/dehydration behavior of hydroxyethyl cellulose ether in aqueous solution, Molecules, 2020, 25 (20), 4726

[49] S. H. Wang, R. D. Singh, L. Godin et al., Endocytic response of type I alveolar epithelial cells to hypertonic stress, American Journal of Physiology Lung Cellular and Molecular Physiology, 2011, 300, 560–568

[50] J. Park, K. Kim, S. Jeong, Hightly osmotic oxidized sucrose-crosslinked polyethylenimine for gene delivery systems, Pharmaceutics, 2021, 13 (1), 87

[51] J. Jeon, J. Park, and T-i. Kim, Phenylboronic acid-conjugated cationic methylcellulose for hepatocellular carcinoma-targeted drug/gene co-delivery systems, Journal of Industrial and Engineering Chemistry, 2019, 75, 148–157

[52] C. Chen, B. Zhou, X. Zhu et al., Branched polyethylenimine modified with hyaluronic acid via a PEG spacer for targeted anticancer drug delivery, Royal Society of Chemistry, 2016, 6, 9232–9239

[53] B. Zhou, L. Zhoa, M. Shen et al., A multifunctional polyethylenmine-based nanoplatform for targeted anticancer drug delivery to tumors in vivo, Journal of Materials Chemistry B, 2017, 5 (8), 1542–1550

[54] C. F. Borgognoni, J. Kim, V. Zucolotto, et al., Human macrophage responses to metal-oxide nanoparticles: a review, Artificial Cell, Nanomedicine, and Biotechnology, 2018, 46 (2), 694–703

[55] S. Mitragotri, P. A. Burke, R. Langer, Overcoming the challenges in administering biopharmaceutics: formulation and delivery strategies, Nature Reviews, 2014, 13, 655–672

[56] Z. Sun, Z. Zhao, G. Li et al., Relevance of two genes in the multidrug resistance of hepatocellular carcinoma: in vivo and clinical studies, Tumori, 2010, 96 (1), 90–96

[57] L. Sun, W. Chen, L. Qu et al., Incaritin reverses multidrug resistance of HepG2/ADR human hepatoma cells via downregulation of MDR1 and P-glycoprotein expression, Molecular Medicine Reports, 2013, 8 (6), 1883–1887

[58] T. C. Chou, Derivation and properties of Michaelis-Menten type and Hill type equations for reference ligands, Journal of Theoretical Biology, 1976, 59 (2), 253–276

[59] T. Zhang, C. Fu, I. Alradwan, et al., Targeting signaling pathways of hyaluronic acid and integrin receptors by synergistic combination nanocomposites inhibits systemic metastases and primary triple negative breast cancer, Advanced therapeutics, 2021, 4 (6) -

[60] M. van Engeland, L. J. Nieland, F. C. Ramaekers et al., Annexin V-affinity assay: a review on an apoptosis detection system based on phosphatidylserine exposure, Cytometry, 1998, 31 (1), 1–9

Abstract in Korean

하이드록시에틸 셀룰로오스 (HEC) 는 생체적합성과 물에 대한 용해도가 뛰어나 전달 시스템과 같은 의용 소재로 활용될 가능성이 있는 물질이다. 본 연구에서는 폴리에틸렌이민 (PEI) 로 개질된 하이드록시에틸 셀룰로오스 (HECP2k) 를 합성하고 유전자 및 약물 동시 전달체로서의 가능성을 평가하였다. HECP2k는 PEI와 산화 하이드록시에틸 셀룰로오스 간의 환원 아미노화 반응에 의해 합성하였다. PEI의 반응비를 달리하여 합성한 고분자를 HECP2k 1X, HECP2k 5X, HECP2k 10X라고 명명하였다. ^{1}H NMR과 1차 아민 정량을 통해 PEI의 반응비가 증가할수록 PEI의 합성 비율 역시 증가함을 확인하였다. GPC를 통해 측정한 상대 분자량은 HECP2k 1X, 5X, 10X 각각 13.92, 9.38, 7.27 kDa 으로 확인하였다.

아가로스 젤 전기영동을 통해 플라스미드 DNA와의 폴리플렉스 형성 능력을 확인하였다. 폴리플렉스의 제타 평균 사이즈와 제타 전위는 DLS를 통해 측정하였고 100–300 nm 의 입자 크기와 +30 mV 정도의 제타 전위를 유지함을 확인하였다. HECP2k 1X 의 경우 약간의 세포 독성을 띠고 있었지만 HECP2k 5X 와 10X 의 경우 무시할 수 있을 정도의 독성을 가짐을 확인하였다. 이후 최적의 고분자/유전자 간의 무게비를 결정하기 위해 유전자 전달 효율 평가를 진행한 결과 대조군인 PEI25k 에 비해 높은 전달 효율을 가짐을 확인하였고, 이후 실험부터는 HECP2k 10X 를 가지고 무게비를 50 으로 하여 진행하였다. 유세포 분석과 공초점 현미경 이미지를 통해 대조군인 PEI25k 에 비해 높은 세포 침투와 우수한 세포

내 거동을 가짐을 확인하였다. 또한 PEI25k 에 비해 높은 세럼 단백질에 대한 안정성을 보임을 확인하였다.

Doxorubicin을 담지한 뒤 약물 로딩 양과 효율을 측정한 결과, 각각 13.83% 와 41.49%로 계산되었다. Bcl-2 siRNA와 형성한 복합체는 HECP2k/siRNA 의 경우 153.7 nm, 14.67 mV, HECP2k@Dox/siRNA 의 경우 241.3 nm, 16.97 mV 의 크기 및 제타 전위를 갖는다는 것을 확인하였다. 다중 약물 내성 (Multi-drug resistance) 이 없는 세포에 반해, 다중 약물 내성이 있는 세포에 대하여 HECP2k@Dox/siRNA 복합체가 갖는 공동 상승 항종양 효과를 확인하였다. 또한 아폽토시스을 유도함으로써 항암 효과를 띤다는 것을 확인하였다. 결론적으로 HECP2k는 높은 세럼 단백질에 대한 안정성, 높은 유전자 전달효율, 향상된 항종양 효과 등의 장점을 가진 Bcl-2 siRNA/Doxorubicin 동시 전달체로서의 새로운 가능성을 제시하였다.